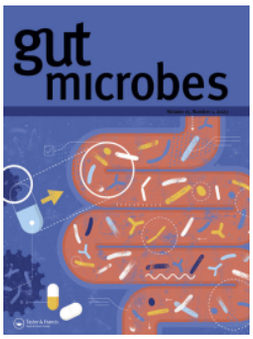

Gut Microbes

ISSN: 1949-0976 (Print) 1949-0984 (Online) Journal homepage: www.tandfonline.com/journals/kgmi20

Blood-borne immune cells carry low biomass DNA remnants of microbes in patients with colorectal cancer or inflammatory bowel disease

Yasser Morsy, Åsa Walberg, Paulina Wawrzyniak, Barbara Hubeli, Luca Truscello, Celine Mamie, Ania Niechcial, Emilie Gueguen, Roberto Manzini, Claudia Gottier, Silvia Lang, Sylvie Scharl, Sena Blümel, Luc Biedermann, Gerhard Rogler, Matthias Turina, Michaela Ramser, Henrik Petrowsky, Isabelle C. Arnold, Sebastian Zeissig, Nicola Zamboni, Adrian Egli, Jan Hendrik Niess, Petr Hruz, Alexander Knuth, Ralph Fritsch, Markus G. Manz, Marcin Wawrzyniak & Michael Scharl

To cite this article: Yasser Morsy, Åsa Walberg, Paulina Wawrzyniak, Barbara Hubeli, Luca Truscello, Celine Mamie, Ania Niechcial, Emilie Gueguen, Roberto Manzini, Claudia Gottier, Silvia Lang, Sylvie Scharl, Sena Blümel, Luc Biedermann, Gerhard Rogler, Matthias Turina, Michaela Ramser, Henrik Petrowsky, Isabelle C. Arnold, Sebastian Zeissig, Nicola Zamboni, Adrian Egli, Jan Hendrik Niess, Petr Hruz, Alexander Knuth, Ralph Fritsch, Markus G. Manz, Marcin Wawrzyniak & Michael Scharl (2025) Blood-borne immune cells carry low biomass DNA remnants of microbes in patients with colorectal cancer or inflammatory bowel disease, Gut Microbes, 17:1, 2530157, DOI: 10.1080/19490976.2025.2530157

To link to this article: https://doi.org/10.1080/19490976.2025.2530157

© 2025 The Author(s). Published with license by Taylor & Francis Group, LLC.

View supplementary material

Published online: 20 Jul 2025.

Submit your article to this journal

Article views: 2069

View related articles

View Crossmark data

Full Terms & Conditions of access and use can be found at
https://www.tandfonline.com/action/journalInformation?journalCode=kgmi20

GUT MICROBES
2025, VOL. 17, NO. 1, 2530157
https://doi.org/10.1080/19490976.2025.2530157

Taylor & Francis
Taylor & Francis Group

RESEARCH PAPER

OPEN ACCESS Check for updates

Blood-borne immune cells carry low biomass DNA remnants of microbes in patients with colorectal cancer or inflammatory bowel disease

Yasser Morsy[a*], Åsa Walberg[a*], Paulina Wawrzyniak[a*], Barbara Hubeli[a], Luca Truscello[a], Celine Mamie[a], Ania Niechcial[a], Emilie Gueguen[a], Roberto Manzini[a], Claudia Gottier[a], Silvia Lang[a], Sylvie Scharl[a], Sena Blümel[a], Luc Biedermann[a], Gerhard Rogler[a], Matthias Turina[b], Michaela Ramser[b], Henrik Petrowsky[b], Isabelle C. Arnold[c], Sebastian Zeissig[d], Nicola Zamboni[e], Adrian Egli[f], Jan Hendrik Niess[g,h], Petr Hruz[g], Alexander Knuth[i], Ralph Fritsch[i,j], Markus G. Manz[i,j], Marcin Wawrzyniak[a*], and Michael Scharl[a,j*]

[a]Department of Gastroenterology and Hepatology, University Hospital Zurich, University of Zurich, Zurich, Switzerland; [b]Department of Visceral and Transplant Surgery, University Hospital Zurich, University of Zurich, Zurich, Switzerland; [c]Institute of Experimental Immunology, University of Zürich, Zurich, Switzerland; [d]Center for Regenerative Therapies Dresden (CRTD), Technische Universität (TU) Dresden, and Department of Medicine I, University Medical Center Dresden, Dresden, Germany; [e]Institute of Molecular Systems Biology, Federal Institute of Technology Zurich, Zurich, Switzerland; [f]Institute of Medical Microbiology, University of Zurich, Zurich, Switzerland; [g]Department of Gastroenterology and Hepatology, University Digestive Healthcare Center, Basel, Switzerland; [h]Department of Biomedicine, Gastroenterology, University of Basel, Basel, Switzerland; [i]Department of Medical Oncology and Hematology, University Hospital Zurich, University of Zurich, Zurich, Switzerland; [j]Comprehensive Cancer Center Zurich, University Hospital Zurich, University of Zurich, Zurich, Switzerland

ABSTRACT

The involvement of the intestinal microbiome in the pathogenesis of inflammatory bowel disease (IBD) and colorectal cancer (CRC), is well-established. Bacteria interact with immune cells at sites of intestinal inflammation, but also in the CRC tumor microenvironment. We hypothesized that bacterial remnants translocate within peripheral blood mononuclear cells (PBMCs) into the circulation and thus explored the composition of the detectable microbiome in PBMCs of patients with CRC or IBD compared to healthy controls. The PBMC microbiome profiles partially align with the tumor-derived or intestinal tissue-derived microbiome signatures obtained from the same patients with CRC or IBD, respectively. Our metagenomics data, supported by 16S-rRNA-FISH-Flow, imaging flow cytometry and species-specific qPCR, revealed the presence of translocated bacterial genetic sequences in the patients with CRC and IBD. Thus, our data suggest that in patients with intestinal barrier leakage, there is the potential for the translocation of bacterial remnants into the circulation via PBMCs.

ARTICLE HISTORY
Received 21 February 2025
Revised 17 April 2025
Accepted 1 July 2025

KEYWORDS
Microbiome; colorectal cancer metastasis; inflammatory bowel disease pathogenesis; cancer and microbiome; intestinal epithelial barrier defect; peripheral blood mononuclear cells; microbiome host interaction

Introduction

The intestinal microbiome is critical for the maintenance of human health as it is an important contributor to effective epithelial barrier function, immune tolerance, energy production, and digestion, as well as the production of vitamins, bile acids, and short-chain fatty acids.[1] The involvement of the human intestinal microbiome in the regulation of immune cell homeostasis, as well as in the pathogenesis of inflammatory bowel disease (IBD) and colorectal cancer (CRC), is well-established.[2–5] Bacteria interact with immune cells at the sites of intestinal inflammation, but also in the CRC tumor microenvironment (TME).[2–7] Indeed, bacterial remnants have recently been detected in human intestinal tissue in patients with IBD, at primary tumor sites and in the metastases of patients with CRC, and in whole blood.[4,8,9]

In patients with IBD, a reduced diversity and metabolic capacity of the intestinal microbiome has been documented.[10–13] Additionally, patients with active IBD present an enhanced intestinal permeability and

CONTACT Michael Scharl michael.scharl@usz.ch Department of Gastroenterology and Hepatology, University Hospital Zurich, University of Zurich, Zurich 8091, Switzerland

*These authors contributed equally to this work.

Supplemental data for this article can be accessed online at https://doi.org/10.1080/19490976.2025.2530157

© 2025 The Author(s). Published with license by Taylor & Francis Group, LLC.
This is an Open Access article distributed under the terms of the Creative Commons Attribution-NonCommercial License (http://creativecommons.org/licenses/by-nc/4.0/), which permits unrestricted non-commercial use, distribution, and reproduction in any medium, provided the original work is properly cited. The terms on which this article has been published allow the posting of the Accepted Manuscript in a repository by the author(s) or with their consent.

increased bacterial DNA load in intestinal tissue compared to healthy controls.[14–16] Thus, it has been hypothesized that the intestinal microbiome affects immune cell homeostasis in patients with IBD and other chronic inflammatory diseases with systemic consequences, either indirectly or directly via the presence of relevant pathogenic bacteria in the periphery, including the circulation.[5] Furthermore, in CRC, the intestinal microbiome is found in a dysbiotic state, and bacteria have been found within the TME.[3,4,8,17–20]

Indeed, several studies have shown the functional implications of such bacterial signatures on cancer progression.[2,18,21] Bacterial genes at primary tumor sites in patients with CRC or oral squamous cell cancer have been observed in cancer and immune cells,[4,8] and regions containing bacterial sequences within the tumor tissue have been associated with an increase in the population of myeloid cells.[4] And, in addition to a detectable microbiome occurring within the primary tumor, it has been shown that CRC-related liver metastases harbor bacteria[8] and strains of *Fusobacterium nucleatum*, *Bacteroides fragilis*, and *Prevotella spp*. have been identified on a genetic level in both the primary CRC tumor and the corresponding liver metastasis.[8] Animal studies have further revealed that a defective intestinal vascular barrier might promote bacterial translocation, thus promoting cancer metastasis.[22]

The hypothesis that commensal bacteria, or at least bacterial remnants, might translocate from the intestine into the circulation through a potentially defective intestinal epithelial barrier in patients with IBD or CRC is corroborated by the highly sporadic detection of bacterial DNA in the blood of healthy individuals. In an elegant study, *Tan et al.* detected genetic sequences from mainly commensal bacteria derived from the intestinal tract, oral cavity or the genito-urinal tract in whole blood samples of 9,770 healthy individuals. The identified sequences differed from known human pathogens in clinical blood cultures.[9] However, bacterial species were recognized in only 16% of those healthy individuals, and the detected median was one species, suggesting that under homeostatic conditions there is an absence of a consistent core microbiome within human blood.[9] However, the overall microbial DNA load in whole blood in patients with CRC or IBD is higher compared to healthy controls, albeit with yet unclear pathological consequences.[23,24]

As of yet it is unknown how bacteria or bacterial remnants can travel systemically and, in particular, reach sites of distant metastases in patients with CRC or sites of localized inflammatory activity in the case of IBD. But, due to the interaction of bacteria with immune and cancer cells at primary tumor sites,[4] we speculated that such bacterial remnants travel either within cancer cells or immune cells from the primary tumor to sites of metastasis. Here, we show that in patients with CRC or IBD peripheral blood mononuclear cells (PBMCs) may carry translocated bacterial remnants into the circulation, likely due to a defect in their intestinal epithelial barrier.[25]

Results

Genetic bacterial sequences are detectable within the PBMCs of patients with CRC or IBD

Firstly, we aimed to explore whether PBMCs might contribute to the translocation of bacterial remnants from sites of primary tumors or from the inflamed intestinal tissue into the blood in patients with CRC or IBD, respectively. We performed metagenomics sequencing on PBMCs derived from 36 patients with CRC, including patients with stages I-III (n = 24) and stage IV (n = 12), and 56 patients suffering from IBD (ulcerative colitis, UC, n = 25; Crohn's disease, CD, n = 31). In addition, we analyzed PBMCs from healthy control individuals (n = 20) (Table S1). To exclude potential contamination affecting the results, we used multiple lab reagent controls (Table S2). We performed extensive bioinformatics data cleaning procedures according to recommended guidelines to avoid potential pitfalls of low-biomass microbial analyses and to recognize the reagent microbiome in our samples (Figure S1A-C, Table S3, Methods).[26,27] Further, we only selected species for further analysis that are well-known to colonize the human gut and are thus ecologically plausible. After performing each step of this data decontamination pipeline, 208 bacterial species (126 in tissue only and 82 in both PBMCs and tissue) were detectable at a rate of at least 10 specific reads in at least 3 patients for at least one disease in either tissue and/or PBMCs (Figure S1A-C, Table S4).We found a higher microbial richness as measured by Chao1 in PBMCs from patients with metastatic and non-metastatic CRC compared to PBMCs from patients with IBD (Figure 1(a), Table S5). Beta diversity analysis based on Bray-Curtis presented by Principal Coordinates Analysis (PCoA) demonstrated a cluster of PBMCs from patients

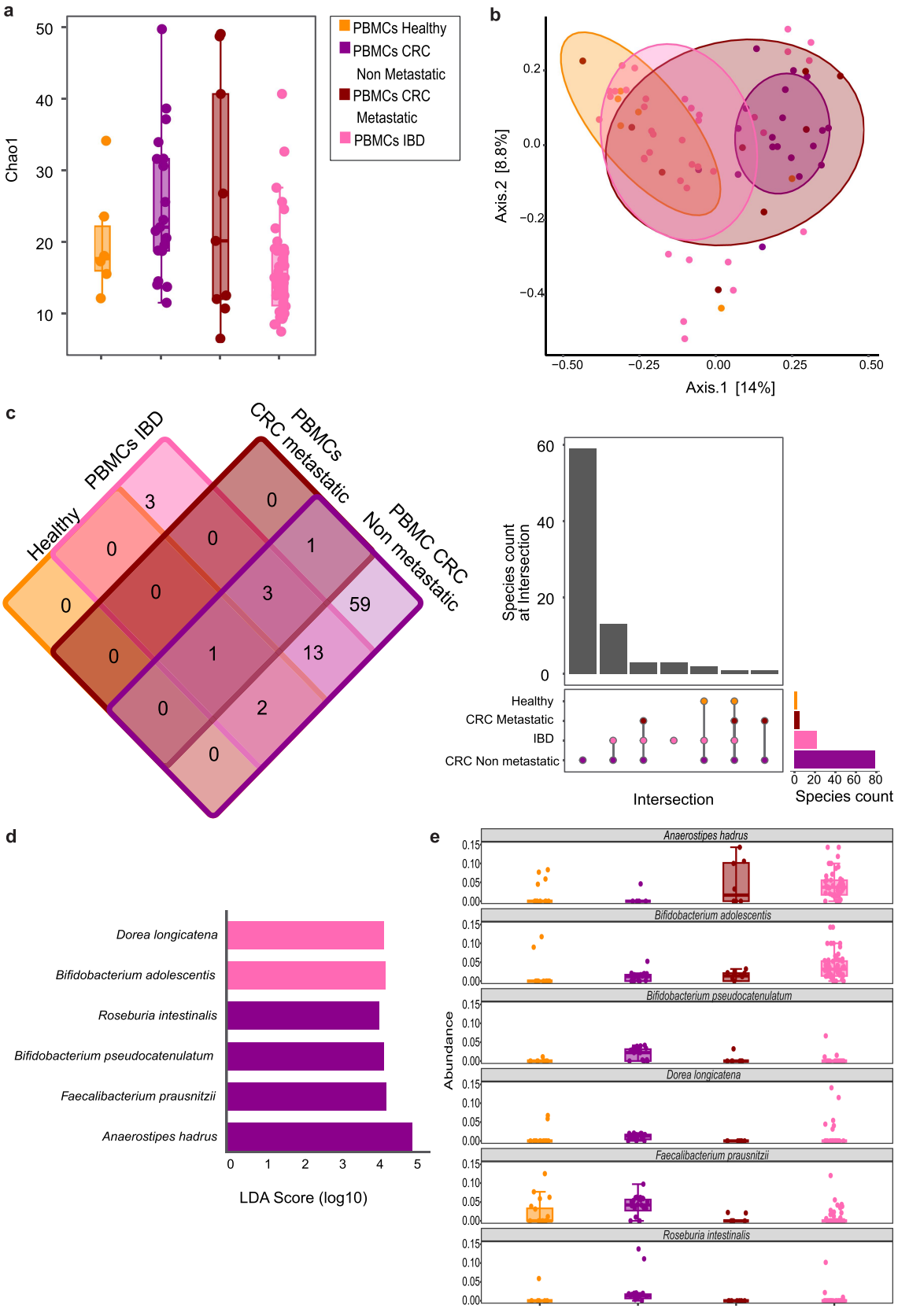

Figure 1. The bacterial profile of PBMCs in patients with CRC, IBD, and healthy controls. Specific samples were removed due to rarefaction, which was conducted to normalize the results. (a) Chao1 alpha diversity index diversity measurements of bacterial taxa were detected inPBMCs from patients with IBD (n=37), CRC non metastatic ($n = 19$), metastatic CRC ($n = 9$), as well as in healthy controls ($n = 6$). Specific samples were removed due to rarefaction normalization. (b) Beta diversity analysis based on Bray-Curtis presented by Principal coordinates analysis (PCoA) showed differences between PBMCs from

with non-metastatic CRC were separated from patients with IBD and healthy control individuals. These results were statistically supported by PERMANOVA analysis (Figure 1(b), Table S6). Further analysis based on stratification of patients with CRC according to tumor stages I-IV as well as of patients with IBD according to UC and CD can be found in Figure S2A-D. Notably, while based on Chao1 alpha diversity, there was no clear correlation between age and the number of bacterial species detected within the PBMCs of younger and older individuals (Figure S3A-G).

After applying our strict filtering and decontamination criteria, we still detected bacterial DNA in the PBMCs from all patients and all healthy controls. To check the commonly detected bacterial DNA in PBMCs between different diseases, we set up a threshold of 10 reads to consider the bacterial DNA as present in each condition (Figure S1D). Therefore, PBMCs from patients with non-metastatic CRC had the highest number of diverse bacterial species (n = 79), followed by IBD (n = 22). In contrast, PBMCs from patients with metastatic CRC (n = 5) exhibited only very few bacterial species, and the lowest number of species was detected in PBMCs from healthy individuals (n = 3) (Figure 1(c), Table S4). Of the three species detected in healthy individuals in our samples, *Anaerobutyricum hallii* and *Haemophilus parainfluenzae* had previously been reported in a comprehensive analysis of the whole-blood microbiome of 9770 healthy individuals,[9] which included extensive filtering for contaminants.

Out of the 82 species detected in PBMCs overall, 31 exhibited a remarkable difference between at least two groups (Figure S4). Further, we could define disease-specific PBMC patterns as determined by the effect size (LDA score, log10, Figure 1(d,e)). *Roseburia intestinalis, Bifidobacterium pseudocatenulatum, Faecalibacterium prausnitzii* and *Anaerostipes hadrus* were distinctive for patients with non-metastatic CRC, while *Bifidobacterium adolescentis* and *Dorea longicatena* were indicative for PBMCs from patients with IBD (Figure 1(d,e)). Notably, *Anaerostipes hadrus* featured a high LDA score for non-metastatic CRC as it was enriched in PBMCs from patients with metastatic CRC or with IBD.

Bacterial DNA is present in specific PBMC subsets from patients with CRC and IBD

Next, we aimed to confirm the presence of bacterial DNA in PBMCs and to determine the specific immune cell subsets carrying bacterial DNA in the peripheral circulation. We integrated the detection of the bacterial 16S rRNA using a fluorescence *in situ* hybridization (FISH) probe into our flow cytometry staining of PBMCs (16S rRNA-FISH-Flow) to further validate our findings (Figures 2(a,b), Figures S5–8). Confirming our previous finding of a very low number of bacterial species detected in PBMCs from healthy controls using metagenomic sequencing, we detected almost no bacterial 16S rRNA signal in PBMCs from healthy controls (n = 9) using 16s rRNA FISH Flow. In contrast, we identified the presence of bacterial 16S rRNA in selective immune cell subtypes of PBMCs from patients with CRC (n = 10), particularly in $CD4^+$ T cells and in $CD3^-CD14^+$ monocytes. When analyzing the PBMCs from patients with IBD (n = 9), we detected bacterial 16S rRNA to an overall lesser extent and primarily within the $CD3^-CD14^+$ monocytes. To further validate our findings, we expanded our analysis and adopted the imaging flow cytometry technique. This method enabled us to visualize cells containing the 16S rRNA gene while simultaneously exhibiting characteristic immune cell markers. In this manner, we confirmed our metagenomics findings and validated the presence of 16S rRNA within specific immune cell populations at a single-cell level Figure 2(c,d).

The bacterial sequences detectable within PBMCs and tumor-derived tissue from patients with CRC suggest translocation of bacterial remnants from the intestine

Having demonstrated the presence of bacterial remnants in PBMCs of patients with CRC and IBD, we next aimed to identify the potential origin of the bacterial species found in the PBMCs. Firstly, we explored patients with CRC from whom either PBMCs, primary tumor, and adjacent colon tissue were available (n = *16* non-

healthy individuals and PBMCs from patients with CRC and IBD. (c) a Venn diagram and an upset plot show the number of common bacterial species in different diseases. (d) Effect size analysis (LDA score, log10) shows different taxa detected in PBMCs from each group, as in A, with an LDA score of more than 3. (e) Relative abundance (normalized to a total of 1) of the six species with LDA score above 3.

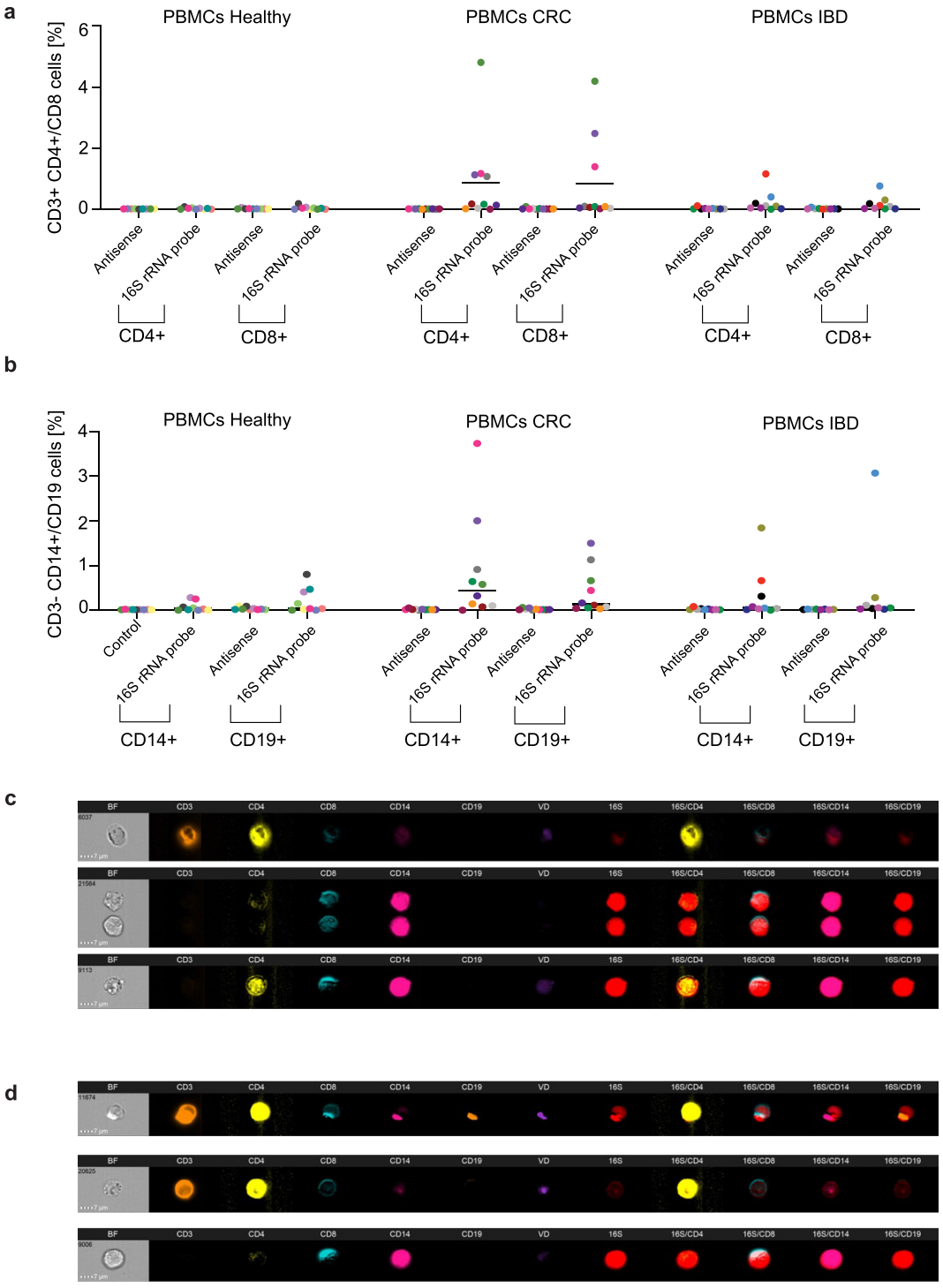

Figure 2. Detection of 16S rRNA-positive cells within total PBMCs from patients with CRC or IBD. PBMCs from healthy controls, $n = 9$, CRC patients, $n = 10$ and IBD patients, $n = 9$ were stained for surface markers CD3, CD4, CD8, CD14 and CD19, and 16S rRNA probe and complementary antisense as a control. These patients had not been previously analyzed by metagenomic sequencing but were included here as an additional validation cohort. (a) Detection of 16S rRNA probe in $CD3^+CD4^+$ T cells and $CD3^+CD8^+$ T cells in comparison to antisense probe. (b) Detection of 16S rRNA probe in $CD3^-CD14^+$ monocytes and $CD3^-CD19^+$ B cells in comparison to antisense probe. Each symbol represents one donor. (c) Representative pictures of PBMCs from CRC donor positive for 16S rRNA probe together with CD3, CD4, CD8 and CD14 cell markers visualized by imaging flow cytometry. (d) Representative pictures of PBMCs from IBD donor positive for 16S rRNA probe together with CD3, CD4, CD8 and CD14 cell markers visualized by imaging flow cytometry. Data is shown as means ± SD, Two-way ANOVA test followed by Bonferroni's multiple comparison test was performed.

metastatic, $n = 4$ metastatic) and patients with CRC from whom PBMCs, metastatic liver and adjacent liver tissue were available ($n = 5$) (Table S1). We observed a markedly higher alpha diversity as measured by Chao1, meaning a higher bacterial richness, in both adjacent colon tissue and tumor tissue from patients with non-metastatic CRC compared to their matching PBMCs (Figure 3(a)). Beta diversity analysis using Bray-Curtis revealed remarkable differences between PBMCs from patients with CRC and matching adjacent colon and primary tumor tissues (Figure 3(b)). Notably, *Anaerostipes hadrus* and *Collinsella aerofaciens* were the most dominant bacterial species in PBMCs from patients with CRC. These species were also detectable in the respective matched intestinal and metastatic CRC tissue, as well as the respective adjacent intestinal and liver tissue (Figure 3C). In contrast, we found that *Haemophilus parainfluenzae, Prevotella sp. E2–28* and *Clostridioides difficile* were the most abundant species in the PBMCs from patients with liver metastasis and their corresponding CRC liver metastatic tissue. Of note, these species were less abundant in the PBMCs from patients with non-metastatic CRC, and they were almost absent in their matching intestinal CRC and adjacent tissue (Figure 3(c)). In contrast, *Bacteroides fragilis* and *Phocaeicola vulgatus* were highly detectable in intestinal CRC and intestinal adjacent tissue, but mostly absent in the PBMCs and the liver tissues. *Fusobacterium nucleatum* was mainly detectable in the intestinal tumor tissue from patients with non-metastatic CRC, but also in the PBMCs of those patients (Figure 3(c)). These patterns suggest distinct translocation profiles of specific bacterial species from the intestine into the PBMCs in patients with CRC. Histological evaluation of adjacent colon and CRC tissues can be found in Figure S9A. Overall, for 82 species we were able to demonstrate remarkable differences in relative abundance between the cancer tissue and their corresponding adjacent tissue compared to the PBMCs from the same patients (Figure S10).

The bacterial profile of PBMCs and intestinal tissue from patients with IBD suggests the translocation of bacterial remnants from the intestine

Next, we aimed to first confirm in patients with IBD our finding in the PBMCs from patients with CRC, and, secondly, we wanted to explore whether the PBMC-derived microbial sequences in patients with IBD might also potentially originate from the intestine. Representative images of the histological evaluation of IBD tissue can be found in Figure S9B. We analyzed a cohort of 11 patients with IBD from which PBMCs, as well as non-inflamed and inflamed intestinal tissue samples, were available (Table S1). By studying alpha diversity as measured by Chao1, we identified a significant difference between non-inflamed intestinal tissue and PBMCs from the same patients with IBD. The bacterial richness was lowest in the PBMCs from these patients, suggesting the presence of more dominant species in such PBMCs than in the tissue (Figure 3(d)). By a beta diversity analysis using Bray-Curtis we revealed a clear clustering between the PBMCs from patients with IBD and non-inflamed tissue from the same patients, while there was again no clear difference between PBMCs and inflamed tissue from the same patients (Figure 3(e)).

As in CRC, we observed that *Anaerostipes hadrus* was the most abundant species in PBMCs from patients with IBD and it was also highly abundant in their inflamed and non-inflamed intestinal tissue (Figure 3(f)). While less abundant overall, *Phocaeicola vulgatus*, *Faecalibacterium prausnitzii*, and *Bacteroides fragilis* were highly abundant in both inflamed and non-inflamed intestinal tissues, and they were found in lower relative abundance in the PBMCs. In contrast, *Haemophilus parainfluenzae* and *Clostridioides difficile* were highly abundant in the PBMCs and the inflamed tissue, but less detectable in the non-inflamed intestinal tissue. In contrast, *Anaerotruncus colihominis* was almost exclusively present in the PBMCs, while *Phocaeicola dorei* and *Bacteroides xylanisolvens* was almost exclusively found in the intestinal tissue (Figure 3(f)).

To further confirm our findings, we next performed species-specific qPCR on the whole DNA samples that were already used for the metagenomics sequencing. However, we did not have sufficient samples left over to determine the presence of bacterial species in paired PBMCs and respective matched tissue samples. Nevertheless, we confirmed the specific presence of *Anaerostipes hadrus*, *Collinsella aerofaciens*, *Faecalibacterium prausnitzii*, and *Bifidobacterium adolescentis* in PBMCs and tissues from patients with CRC and IBD, respectively (Figure 3(g), Figure S11 + 12, Table S7). These data further support the notion that the translocation of remnants of intestinal bacteria into the PBMCs occur in patients with an underlying intestinal barrier defect.

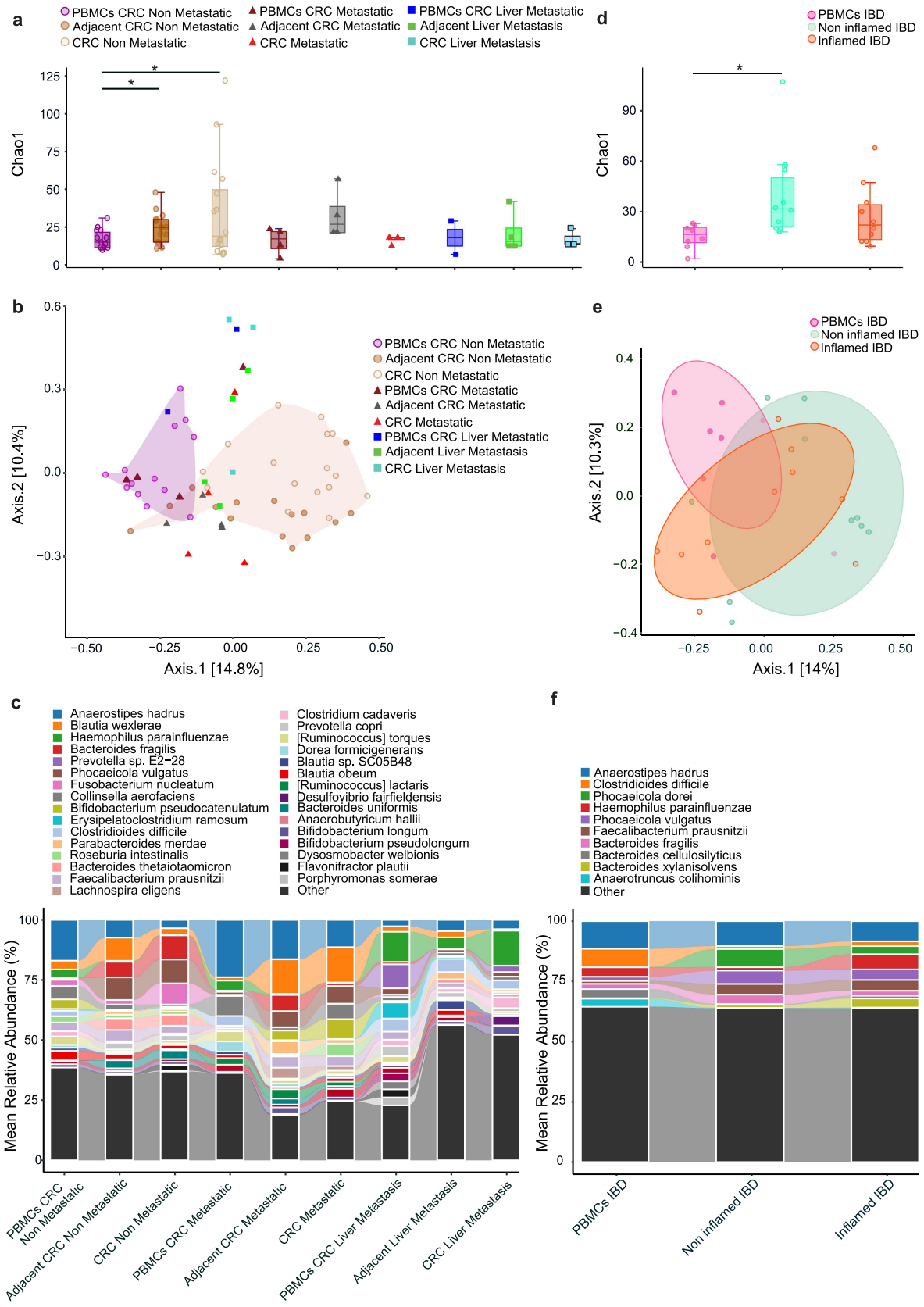

Figure 3a. Bacterial profiles of PBMCs and corresponding tissue samples from the same patients from a cohort of patients with CRC or IBD. Specific samples were removed due to rarefaction, which was conducted to normalize the results. (a) Chao1 diversity index analysis between PBMCs ($n = 20$ and 8 samples excluded), corresponding adjacent colon tissue and CRC tissue from the same patients ($n = 20$ and 5 samples excluded), PBMCs from patients with

A different pattern of bacterial remnants is detectable in PBMCs and intestinal tissue or tumor tissue between patients with CRC and IBD

When comparing all CRC and IBD samples, alpha diversity analysis using the Chao1 metric indicated variations in microbial diversity across different groups (Figure 3(a–d)). Notably, PBMCs from patients with metastatic CRC exhibited a relatively high alpha diversity compared to patients with non-metastatic CRC or IBD. We observed marked differences in the abundance of specific microbial species among the groups (Figure 4(a,b)). For instance, *Prevotella sp. E2–28* and *Fusobacterium nucleatum* were highly abundant in tissue samples from patients with CRC. Conversely, *Vescimonas coprocola* and *Simiaoa sunii* showed a low abundance in these tissues and were almost absent in the PBMCs. Notably, species such as *Faecalibacterium sp. L3839* and *[Ruminococcus] lactaris* were highly abundant in metastatic tissues. The most abundant species, however, including *Phocaecola vulgatus* and *Anaerostipes hadrus*, showed a varied distribution across the groups, indicating their ubiquitous presence.

Metabolite profiling and metagenomics sequencing analysis support the functional relevance of the PBMC-microbiome interaction in patients with CRC and IBD

Next, we aimed to further delineate the potential functional relevance of the PBMC-derived microbiome in patients with CRC and IBD. We applied untargeted metabolomics to profile serum metabolites accounting for the metabolic potential of the detected microbes. We obtained serum from 28 patients with CRC (stages I-III $n = 19$, stage IV $n = 9$), 12 patients with IBD, and 10 healthy control individuals, all with a previously analyzed PBMC microbiome. We observed distinct differences in the metabolite profile of patients with CRC and IBD compared to healthy controls (Figure 5(a)). A total of 635 metabolites were significantly different between the three groups, and differentially regulated metabolites showed an apparent clustering in the heat-map (Figure S13, Table S8). We noted differences for 445 metabolites between patients with IBD and healthy individuals, for 539 metabolites between patients with CRC and healthy individuals, and for 80 metabolites between patients with IBD and CRC. Metabolites altered in either patients with CRC or IBD were used in Metabolite Set Enrichment Analysis (MESA) and pathway analysis, highlighting key metabolic pathways affected in these two patient groups. Here, we observed a disease-specific enrichment, or at least partially, of specific classes of metabolites, including isothiocyanates, diazines, pyrimidine nucleotides, lactones, and benzenes (Figure 5(b)). Pathway enrichment analysis indicated that most of the altered metabolites were involved in phenylalanine, tyrosine, and tryptophan biosynthesis, linoleic acid metabolism, histidine, starch, and sucrose metabolism (Figure 5(c)). Next, we performed a correlation network

metastatic CRC ($n = 4$ and one sample excluded), and PBMCs from patients with CRC liver metastasis, corresponding adjacent liver tissue and CRC liver metastatic lesion from matched patients ($n = 5$ and 3 samples excluded). (b) Beta diversity as assessed by Bray Curtis analysis. (c) Mean relative abundance of most abundant bacterial species pattern across PBMCs and different CRC tissue. (D) Chao1 diversity index analysis between PBMCs ($n = 11$ and 3 samples excluded), corresponding non-inflamed colon tissue, and inflamed tissue from the same patients ($n = 11$ and one sample excluded). (e) Beta diversity assessed using the Bray Curtis analysis. (f) Relative abundance of most abundant bacterial species pattern across PBMCs and different colon tissue from patients with IBD. (g) Detection of *Anaerostipes hadrus*, *Bifidobacterium adolescentis*, *Collinsella aerofaciens* and *Faecalibacterium prausnitzii* with qPCR on whole DNA isolates from PBMCs from CRC patients ($n = 7$, in at least 4/7 patients, DNA was detectable, except for *Bifidobacterium adolescentis*), adjacent CRC ($n = 13$, in least 6/13 patients, DNA was detectable, except for *Bifidobacterium adolescentis*), tumor tissue from CRC patients ($n = 10$, in at least 4/10 patients, DNA was detectable, except for *Bifidobacterium adolescentis*), PBMCs from patients with CRC liver metastasis ($n = 4$, in at least 1/4 patients, DNA was detectable, except for *Bifidobacterium adolescentis*), adjacent liver tissue from patients with CRC liver metastasis ($n = 4$, in at least 1/4 patients, DNA was detectable, except for *Anaerostipes hadrus*), liver metastasis tissue from patients with CRC liver metastasis ($n = 4$, in all 4 patients, DNA was n.D.), PBMCs from IBD patients ($n = 8$, in at least 3/8 patients, DNA was detectable, except for *Faecalibacterium prausnitzii*), non-inflamed IBD colon tissue ($n = 8$, in at least 2/8 patients DNA was detectable) and inflamed IBD colon tissue ($n = 9$, in at least 3/9 patients, DNA was detectable) and PBMCs from healthy controls ($n = 4$, in all 4 patients, DNA was n.D.). In G PBMCs and tissues samples were not derived from the same patients. Data are presented as log10 transformed predicted bacterial DNA concentrations in ng, based on standard curve values generated from pure bacterial DNA of the respective species (Figure S10). n.D. = not detectable.

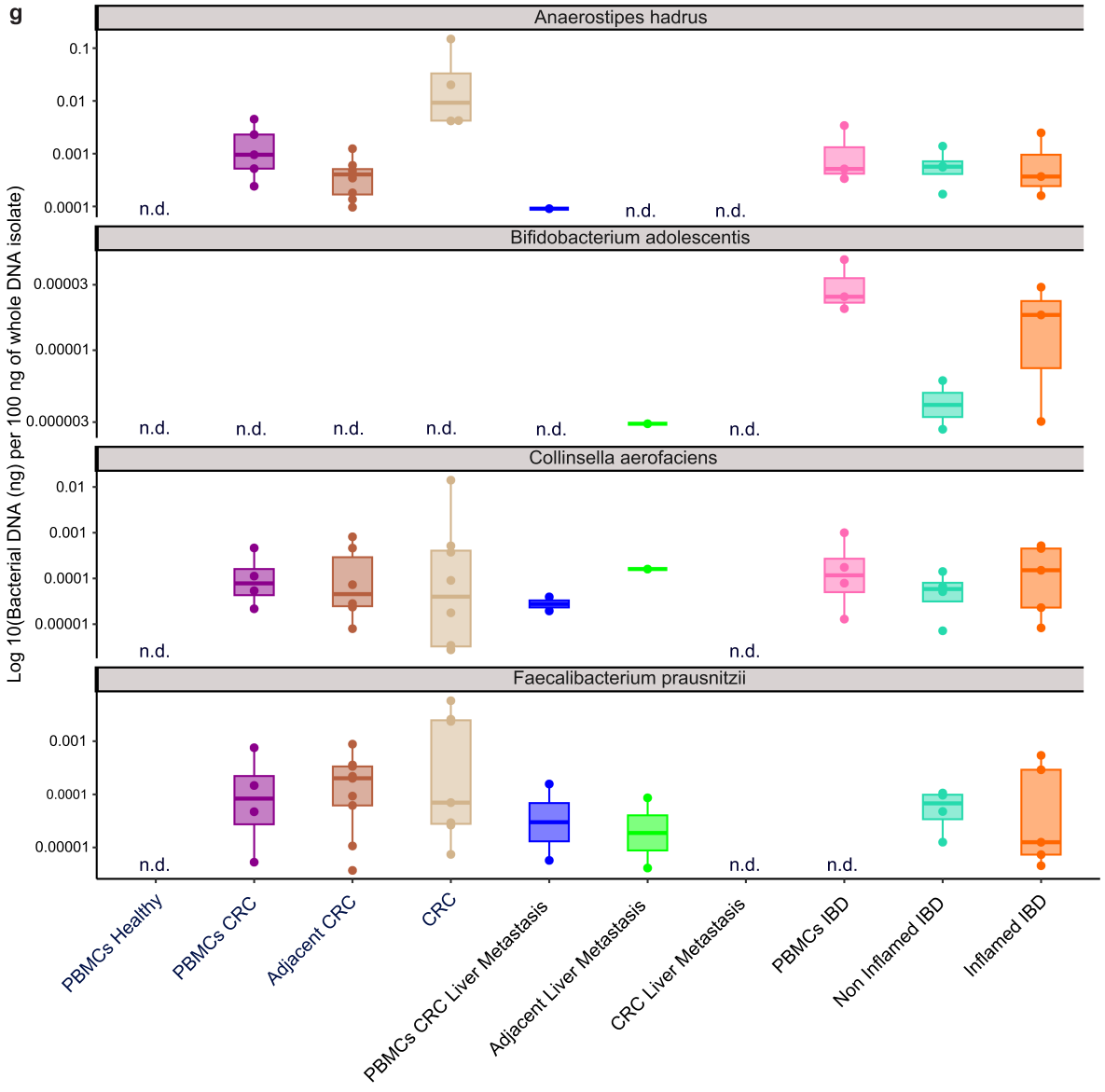

Figure 3b. (Continued).

analysis between altered serum metabolites in patients with CRC and IBD and pathways from corresponding PBMC metagenomics functional analysis data. This analysis revealed that in particular ketogenesis was highly positively correlated, and that plasmalogen degradation was clearly negatively correlated, with the detected serum metabolites (Figure 5(d,e) Tables S9–10).Additionally, we analyzed the significant correlations between PBMC-associated bacterial taxa and serum metabolites from patients with IBD or CRC compared to healthy controls (Figure S14).

Discussion

Here, we provide evidence for a genomic bacterial pattern present within circulating immune cells in the peripheral blood of patients with CRC and IBD. Our data further suggest that the PBMC-derived microbial sequences are likely the result of bacterial translocation from the intestine, particularly in patients with an underlying defect in the intestinal epithelial barrier, which commonly occurs in CRC and IBD.

The role of the microbiome in the pathogenesis of chronic inflammatory and malignant diseases is becoming increasingly evident.[2–5] Recently, it has been demonstrated that primary tumors, as well as metastasis, from patients with CRC exhibit bacterial genetic sequences[4,8]; however, the means by which

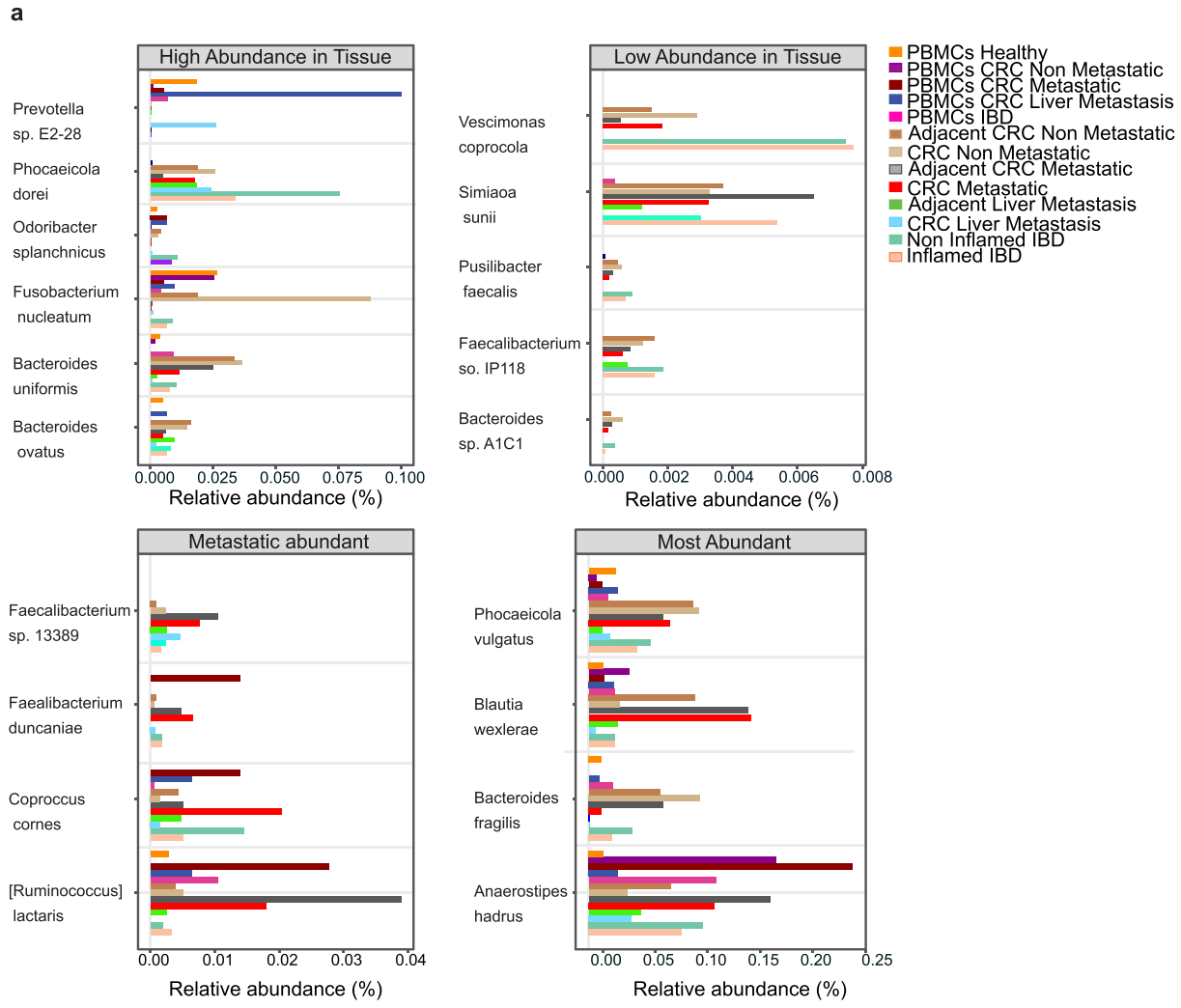

Figure 4. Comparison of bacterial species detected in patients with CRC or IBD in contrast to PBMCs from healthy controls. (a) Histograms show the relative abundance (%) of bacterial species categorized as high tissue abundant (> 0.02%), low tissue abundant (< 0.02%), metastatic abundant (> 0.02%), and most abundant (> 0.02% in both tissue and PBMC samples), with each bar representing the mean relative abundance for each species across different sample types. (B) correlation heatmap of bacterial species represented in Figure 4(a) between samples from CRC metastatic tissue and PMBCs. Only significant correlations with p-values less than 0.05 and Spearman correlation above 0.5 are represented by a pie diagram, and blank squares are insignificant.

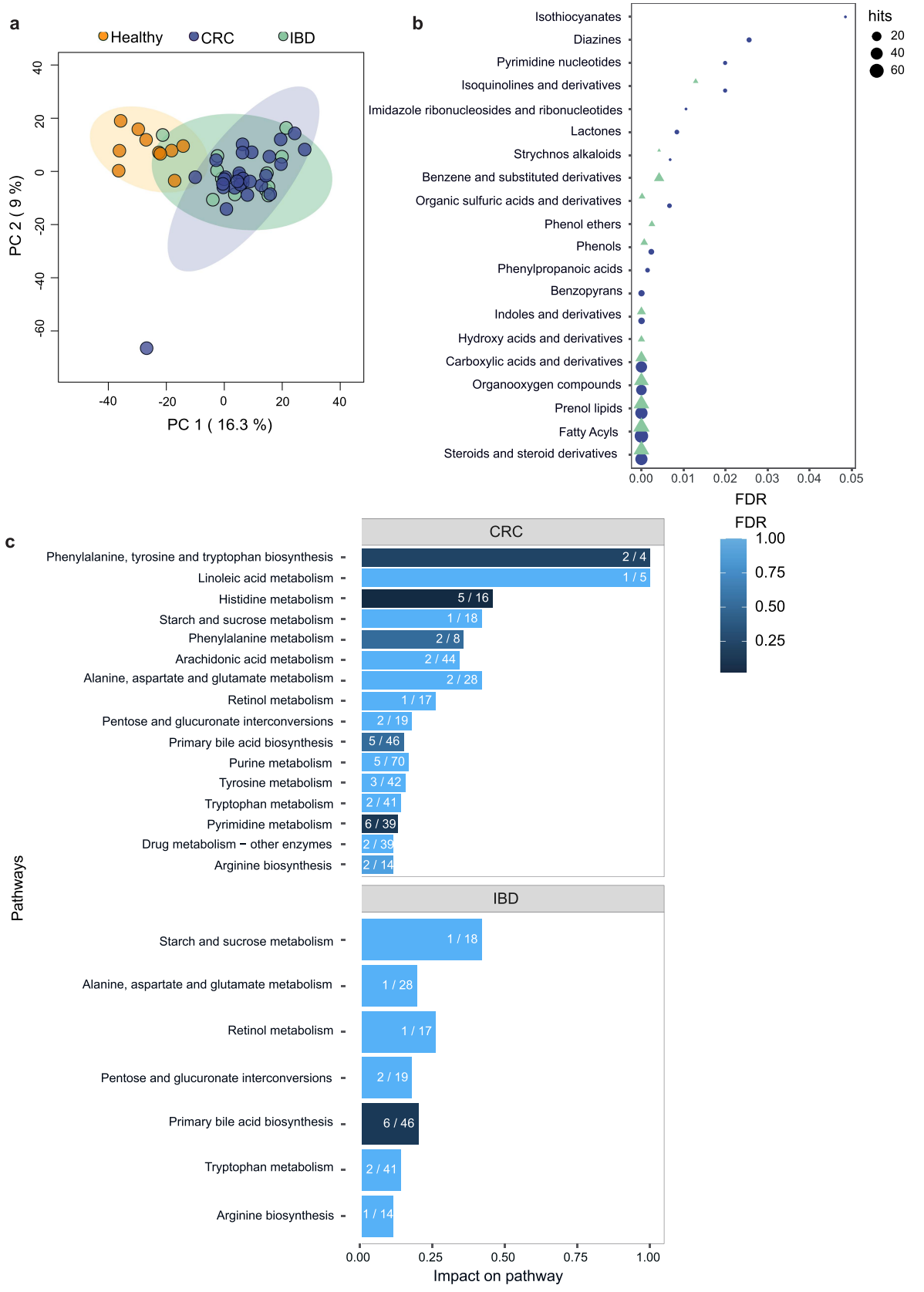

Figure 5a. The serum metabolite profile of a cohort of patients with CRC or IBD and in healthy controls. (a) Principal component analysis (PCA) of serum metabolites in patients with CRC (n = 28), IBD (n = 12), and healthy controls (n = 10). Each dot represents one patient. (b) Metabolites set enrichment analysis of 524 common altered metabolites compared to healthy. (c) Pathway analysis of the detected metabolites. (d) Correlation network between metabolites detected in serum

these bacterial remnants might be transported from the primary tumor to the sites of metastasis, *e.g.*, in the liver, is still unclear. Our data support the concept that in patients with CRC, PBMCs might serve as carriers of bacterial remnants from the intestine and the primary tumor, respectively, toward the sites of metastasis. This data is also in line with the known pro-metastatic roles of certain immune cells recruited to the tumors.[24]

Our data is of interest because, to date, the presence of bacteria in human immune cells has only been described in the context of infectious diseases. Pathogenic *Salmonella* or *Mycobacteria* species can invade and proliferate within dendritic cells and/or macrophages.[28,29] Further, in mouse models of obesity, live bacteria have been shown to translocate from the intestine to adipose tissue via the microbial pattern receptor CD14.[30] In CRC and oral squamous cell cancer bacterial sequences have been detected intracellularly in both the cancer cells and the immune cells of the primary tumors.[4,8] In patients with CRC, *Fusobacterium nucleatum* has been detected in the primary tumor tissue in the intestine, as well as in the liver metastasis[8] and was additionally suggested to reach tumors via the blood.[31] To date, however, the presence of bacteria or bacterial remnants has not been described in circulating PBMCs from patients with CRC or from those with IBD. Thus, this may be a potential means by which bacterial remnants are transported to and end up in peripheral tissues and metastases.

We should note that we observed differences between the microbiome of PBMCs from patients with CRC and IBD. The detected differences in bacterial relative abundances in samples of the same cell type, processed at a single sequencing center, analyzed with the identical pipeline and following the recommendations for reagent microbiome detection, provide substantial evidence that these dissimilarities indeed originate from biological variations and not from recently described technical limitations.[26,27,32] To support our observation, we further confirmed the detection of bacterial sequences in PBMCs from patients with CRC and IBD using a well-established 16S rRNA FISH probe (EUB338).[33,34] Thus, our data demonstrate at least the presence of translocated bacterial genetic sequences, likely bacterial remnants, within the PBMCs of patients with CRC or IBD. Thus, the observed presence of the detected bacterial sequences (regardless whether this indicates the presence of live or dead bacteria) might have an impact on immune cell function and thus on disease pathogenesis, which would be crucial to investigate in future studies.

We also recognized a higher species count for PBMCs from cases of non-metastatic CRC *vs*. those from cases of metastatic CRC, which at first glance seems counter-intuitive within the context of our bacterial translocation model as it would suggest an increased barrier impairment as the adenocarcinoma progresses would lead to potentially greater bacterial translocation. One potential explanation might be, however, that patients with metastatic CRC may have a compromised immune function due to advanced disease or treatments like chemotherapy, which could impact bacterial translocation or its recognition by the immune system.[35] Additionally, changes in the gut microbiota composition toward an even further reduced diversity as the disease progresses might affect the diversity of bacteria available for translocation and thus result in reduced diversity even in the PBMCs, suggesting the presence of fewer, but more dominant, species than in the PBMCs of patients with early-staged CRC.[36] This hypothesis is reflected in our data where in PBMCs from patients with liver metastasis there is a high abundance of bacteria, such as *Haemophilus parainfluenzae*, *Prevotella sp. E2 – 28*, *Erysipelatoclostridium ramosum* or *Clostridioides difficile*, which are clearly less abundant in PBMCs of patients with early-staged CRC.

This concept of reduced diversity might also account for the observed overall trend that younger patients exhibited a higher Chao1 diversity within their PBMCs than older patients. This was especially pronounced in healthy individuals, as well as in patients with metastatic CRC, and indeed a somewhat surprising observation as one might expect that the intestinal barrier is more effective in young people than in elderly people.[37] As an explanation, one might speculate that the highly diverse intestinal microbiome being present within the intestine of younger people might allow for sporadically more diverse bacterial remnants

samples from patients with CRC non-metastatic and altered pathways from metagenomics functional analysis of PBMC samples from patients with CRC non-metastatic. (e) Correlation network between metabolites detected in serum samples and altered pathways resulted from metagenomics functional analysis of PBMC samples from patients with IBD. Only significant correlations with p-values less than 0.05 and Spearman correlation above 0.5 are represented by dark blue lines and less than – 0.5 by light blue lines.

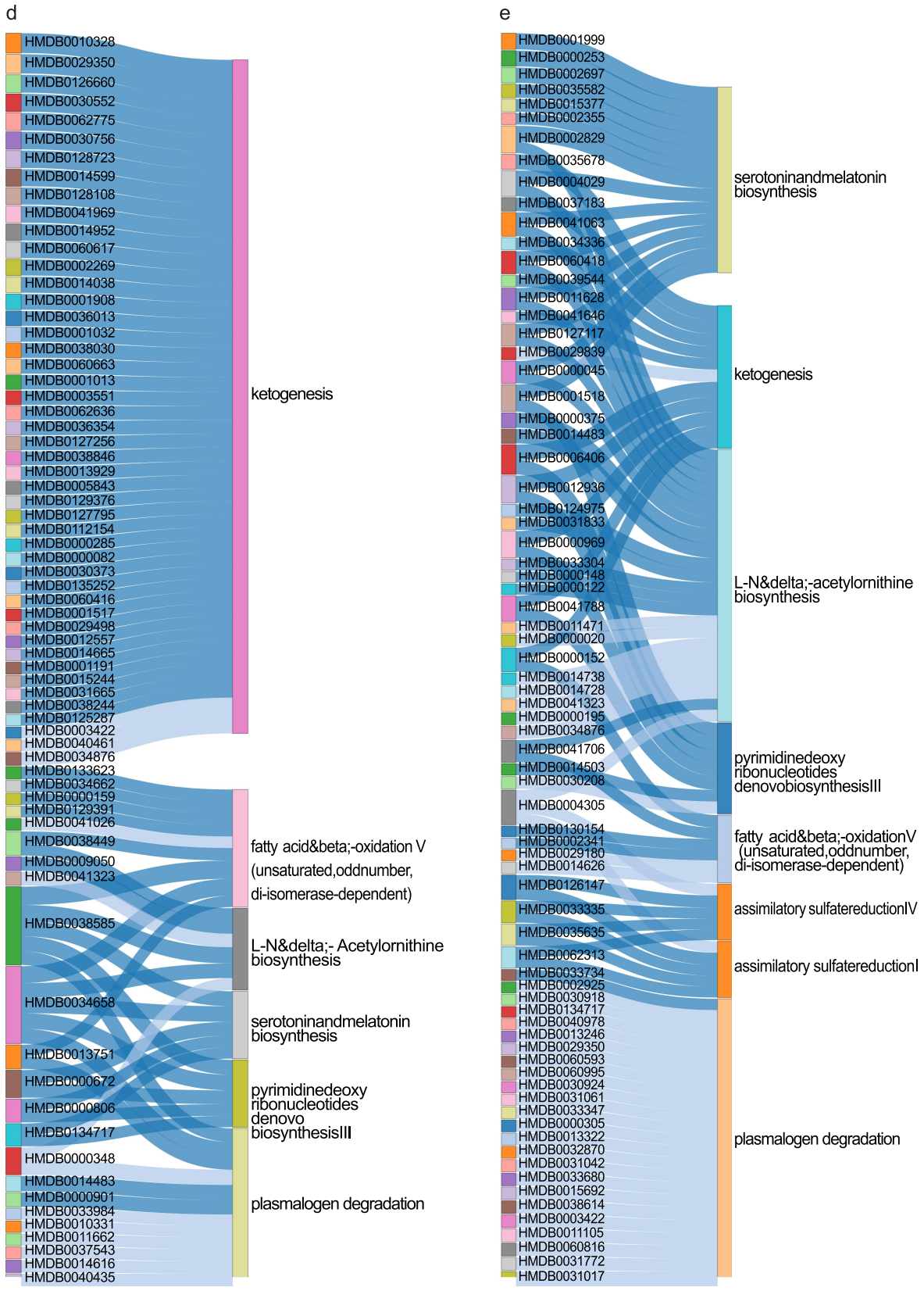

Figure 5b. (Continued).

to pass through the intestinal barrier than in older patients. The microbiome of elderly patients is characterized by clearly less diversity and thus likely more dominant, and also potentially more pathogenic, bacterial species.[38] Thus, such more dominant bacterial species might translocate primarily through the corrupted intestinal barrier into the PBMCs, leading to the greater detection of more dominant species within the PBMCs of the elderly participants in our study. Such a mechanism could also occur in patients with CRC and liver metastasis, where we indeed found higher abundances of dominant, species, such as *Haemophilus parainfluenzae*, *Prevotella sp. E2 – 28* or *Clostridioides difficile*. Thus, the presence and translocation of such dominant species would overrule the effect of a disrupted barrier in elderly people. In patients with IBD the effect of a pronounced dysbiosis in elderly patients compared to younger patients might be somewhat limited as IBD *per se* is characterized by a heavy dysbiosis independent from the patient's age.[39] However, we should note that our cohort was very small to address such differences on a statistically relevant level and further and extensive research beyond the scope of this study would certainly be required to address this issue in detail. Additionally, larger studies would allow for more robust subgroup analyses of both, IBD and CRC, given the high heterogeneity of these diseases.

In our metagenomics data analysis we have strictly adhered to the guidelines for data decontamination in low-biomass microbial studies and paid also particular attention to the recognition of the reagent microbiome in our samples.[26,27] In this way, we aimed to ensure that we did not face recently described problems in certain, mostly cancer-related, microbiome studies.[32] Thus, having performed such stringent contamination removal from our data, our data are now in contrast to previous literature in the field. Notably, many of the previous studies reporting a microbiome within the blood or the tissue of various tumors did not perform such rigorous data decontamination, nor did they report findings that are problematic from an ecological perspective and/or exhibit a high abundance of non-human commensal *Proteobacteria* and finally also commonly contradicting themselves, as, for example, discussed by Ghihawi et al. [32] In particular, some of those publications report a broad amount of *Proteobacteria*, *e.g.*, *Sphingomonadaceae* or *Caulobacteraceae*, which are typical environmental and not human commensal bacteria.[32] Such reported overrepresentation of environmental *Proteobacteria* in the blood or tumor tissue is most likely due to insufficient/incomplete data decontamination and thus recognition of a reagent microbiome, thus denying a common blood microbiome. It also does not make sense from a biological/ecological perspective, given that *Bacteroidetes*, *Firmicutes* and *Actinobacteria* are the main phyla found in the human intestine[40] and the source of detected bacterial remnants in human blood/PBMCs is likely the intestine in individuals with an impaired intestinal epithelial barrier. Further, additional questions arise regarding the validity of such findings in many of the previous studies as bacterial sequences had even been described in cancers of sterile tissues.

We should also note that we detected some uncommon immune cell marker combinations, *e.g.*, $CD3^{-}CD4^{+}$ cells, $CD4^{+}CD8^{+}$ double-positive cells, and also $CD8^{+}CD14^{+}$ double-positive cells. However, those marker combinations have particularly been demonstrated to play a role in immune responses to bacterial antigens and/or the immune response in patients with cancer or chronic inflammatory diseases.[41–46] We detected only a limited number of sequences from bacterial species that are well-known to reside within the human intestine, which further contradicts the notion that the detection of the bacterial sequences by our metagenomics analysis is a result of erroneously assigned human reads in metagenomics sequencing data.[32] Hence, collectively, our data indeed support the presence of at least bacterial remnants in blood cell compartments.[9,23,47]

On a functional level, we have recently demonstrated that some of those identified bacteria, *e.g.*, *Roseburia intestinalis* or *Faecalibacterium prausnitzii*, indeed affect anti-tumor immunity *in vivo* [17] *and those effects are mediated by metabolites produced from those bacteria targeting immune cells via activation of the GPR84 receptor* [48]. *Anaerostipes hadrus*, which proved to be highly detectable in both the PBMCs and intestinal tissue from patients with CRC, was identified in a recent study as a critical modulator of the metabolism of 5-fluorouracil, which is a state-of-the-art chemotherapy for the treatment of CRC. This suggests an important role for this bacterium in patients with CRC.[49] All three of these bacteria have been shown to be highly reduced in the feces of patients with CRC,[17] but are present here at high levels in the primary tumor tissue and, at least on a genetic level, in the PBMCs of those patients. A further validation of our data is the fact that we identified *Fusobacterium nucleatum* at high levels in the primary tumor tissue of

patients with CRC, but not in the intestine of patients with IBD, and at low levels again in PBMCs from patients with CRC and CRC liver metastatic tissue.

By focusing on the distinct bacterial species present in the intestine-derived tissue, as well as the corresponding PBMCs, from patients with IBD and CRC, respectively, we found characteristic patterns for a relevant number of species that might be closely related to their respective functionality. In the intestinal tissue from patients with IBD and CRC, but not in their PBMCs, we detected a high abundance of *Ruminococci*; *e.g.*, the mucolytic *Ruminococcus torques*, *Bacteroides fragilis* or *B. uniformis*. Such mucus degradation might aggravate the defect in the intestinal barrier, allowing additional bacteria to penetrate deeper tissue layers. Correspondingly, we detected a high abundance of various *Lachnospiraceae*, such as *Anaerostipes hadrus, Blautia wexlerae* or *Roseburia intestinalis*, and *Faecalibacteria*, in the intestinal tissue, but also in the PBMCs of those patients. Notably, in PBMCs from patients with a severe intestinal barrier defect; *i.e.*, patients with active IBD and metastatic CRC, we detected high abundances of pathogenic bacteria, such as *Clostridioides difficile* or *Haemophilus parainfluenzae*. These observations are in line with the recent identification of systemic anti-microbiota IgG repertoires, indicating bacterial translocation from the intestine in patients with IBD.[50]

The key novelty of our work is the identification of bacterial sequences in PBMCs of patients with CRC and IBD, as previous studies only focused on the microbiome of fecal, tissue or whole-blood samples, but not on peripheral immune cells. Though our study is limited by the lack of matching primary CRC tissue and corresponding CRC liver metastasis tissue from the same patients due to clinical limitations. Nevertheless, our data demonstrate the presence of a limited number of bacterial sequences that are common to the colonic primary tumor, the PBMCs from patients with CRC and the metastatic CRC liver lesions. Additionally, the overlap of bacterial species found in adjacent colon tissue, in CRC tissue, inflamed IBD tissue, and in PBMCs from patients with CRC and IBD, respectively, potentially suggests a translocation of bacterial remnants, possibly due to increased permeability of the gut barrier as described for CRC and IBD.[51–53] A further limitation that could not yet be addressed in our present study is whether the detected bacterial genetic sequences in PBMCs might be derived from live bacteria. Nevertheless, even if we do not find any evidence of live bacteria in the samples from patients with CRC, especially metastatic CRC, in the future, the overall relevance of our findings will not suffer as it is well possible that bacterial remnants could still have important immunomodulatory effects on CRC and IBD disease course and treatment.[54–56]

Overall, we provide evidence here for the presence of bacterial remnants in circulating immune cells of patients with CRC and IBD. The comparison between PBMCs and the corresponding tissue samples from the same patients identified some common bacterial species, indicating potential mutual microbial signatures, suggesting that a bacterial translocation from the intestine might be the source of the microbial sequences detected in the PBMCs of patients with CRC or IBD (Figure S15). Our findings contribute to the understanding of the complex pathogenesis of CRC and IBD and raise the possibility that the presence of microbial remnants in PBMCs might exert a potential mechanistic role in the pathogenesis of such diseases.

Star methods

Study participant details

Patient recruitment

We included patients diagnosed with either IBD or CRC. In total, 36 patients with CRC were enrolled, comprising 24 patients with stages I – III and 12 patients with stage IV disease. Additionally, 56 patients with IBD were included, of whom 25 had UC and 31 had CD. From the CRC cohort, matching PBMCs, primary tumor tissue, and adjacent normal colon tissue from the same patient were collected from 20 patients ($n = 16$ non-metastatic; $n = 4$ metastatic). Furthermore, a separate cohort of 5 metastatic CRC patients was included, from whom PBMCs, metastatic liver tissue, and adjacent non-tumorous liver tissue were obtained from the same patient each. For the IBD group, matched PBMCs, inflamed, and non-inflamed intestinal tissue were available from the same patient from 11 patients. All CRC patients included were diagnosed with Union for International Cancer Control (UICC) stages I-IV and a minimum of 18 years of age. Additionally, 20 healthy control individuals

were included. Ethical approval for collecting and analyzing tissue and blood specimens from patients with CRC or IBD and healthy control individuals was received by the Cantonal Ethics Committee of the Canton Zürich (BASEC-No.: 2022–02036, BASEC-No.: 2019–02277, EK-1755/PB_2019–00169). Patients were recruited either from the University Hospital Zurich (USZ) or from the University Hospital Basel (USB). All participants provided written informed consent before sample collection due according to local standards and according to the ethical approvals/study protocols. The control subjects were healthy individuals, e.g. undergoing CRC screening or blood donation at the Blood Donation Center, SRK Zurich, Switzerland. Control subjects were not formally age-matched. All samples from patients with CRC or IBD were taken after diagnosis, meaning that all patients had a confirmed diagnosis at the time of biosampling. Samples from patients with CRC were usually taken at time of cancer surgery. Samples from patients with IBD were taken during disease course. Once collected, the samples were treated identically between cases and controls with respect to timing, shipping, lab handling, processing. Disease, age and gender of the participants are provided in Table S1. Additional patient information (e.g. sex, ancestry, race, ethnicity, socioeconomic status, and antibiotic treatment) is not available as per the relevant ethical approvals under which the patients were included.

Method details

Tissue preparation

After surgical resection of human tissues, specimens were assessed by a pathologist. Tumor samples, inflamed and adjacent colon or liver samples were identified by the pathologist. Native tumor tissue and adjacent colon and liver tissue were temporally kept in sodium chloride (NaCl) until snap frozen in liquid nitrogen and stored at −80°C.

Histology

For histological analysis, adjacent colon tissue, tumor, and IBD tissue samples were fixed in 4% formalin (Formafix Switzerland AG 01–1000), dehydrated through a graded ethanol series (70–100%), and embedded in paraffin. Sections of 5 µm thickness were prepared using a rotary microtome (Zeiss Hyram M 15). For further processing, tissue sections were deparaffinized with Histo-Clear (Chemie Brunschwig/National Diagnostics, HS-200) and rehydrated through a descending ethanol series (100–70%). For hematoxylin and eosin (H&E) staining, rehydrated sections were stained with hematoxylin (Roth, 9192.1) for 10 minutes, briefly differentiated in 1% HCl (vwr, 1.00317.1000) in ethanol for 2 seconds, and counter-stained with 1% eosin (Waldeck GmbH & Co, 1B–425, pH 5.2) for 15 seconds. Finally, sections were dehydrated through ascending ethanol concentrations (70–100%) and mounted with Pertex (Biosystems Switzerland AG, 41–4012–00).

Isolation of human PBMCs

Peripheral blood was collected in ethylenediaminetetraacetic acid (EDTA) (Beckton Dickinson (BD), 367525)-containing tubes and was processed within 1–2 h of blood draw. PBMCs were isolated using density gradient centrifugation with Pancoll-Paque at 1.077 g/mL (PanBiotech, PANP04–601000). Briefly, blood was diluted with 2% Fetal Calf Serum (FCS) (Biowest, #S181T) in Phosphate-Buffered Saline (PBS) (ThermoFisher 10,010,056) and gently transferred on top of the density gradient medium layer in SepMate tubes (Stemcell 85,450). Samples were centrifuged at 1000 x *g* for 10 minutes at room temperature (RT), 22°C with the brake on 7. The resulting layer of mononuclear cells was transferred to a new tube, washed with 2% FCS in PBS, and centrifuged at 600 x *g* for 15 minutes with the brake on 7, at RT, followed by one additional wash with 2% FCS in PBS at 300 x *g* with the brake on 7 for 10 minutes. In FCS, cells were frozen in 10% dimethyl sulfoxide (DMSO) (Sigma-Aldrich 41,640) and stored at −80°C.

Infection of human PBMCs with E. coli

The PBMCs were plated in 6-well plate (5 ×106 cells in 5 ml RPMI medium, Gibco) overnight at 37℃ in 5% CO2 atmosphere. Next, PBMCs were treated with antibiotics (gentamicin (100 µg/ml), doxycycline (5 µg/ml)) as a control or infected with different MOI (0, 0.5, 1, 2) of *E. coli* for 2 h. After infection, PBMCs were collected and washed three times with PBS and followed the 16S rRNA FISH staining.

16S rRNA FISH staining

The PBMCs were washed three times with PBS. Next, cells were stained for zombie violet fixable viability dye (Biolegend) 30 min at 4℃, and permeabilized for 20 min at 4℃ with intracellular staining permeabilization wash buffer and fixation buffer (Biolegend). Next, cells were washed with 2x saline-sodium citrate (SSC) buffer (20x SSC buffer, Roth, 1054.1) and stained with a 16Ss rRNA FISH probe EUB338 (5'-GCTGCCTCCCGTA-GGAGT-3), Cy5 (Microsynth) or an antisense probe (5'-ACTCCTACGG-GAGGCAGC-3'), Cy5 (Microsynth) in hybridization buffer (25% formamide Huberlab, A2156.0500), 10% dextran sulfate (ThermoFisher 15,415,089), 0.5% bovine serum albumin (BSA) (Pan-Biotec, PANP06–1391500), 2x SSC buffer) and incubated overnight at 37℃ in 5% CO_2 atmosphere. Next, cells were washed with 2x SSC buffer. After washing with MACS buffer (Miltenyi Biotec 130,091,221) cells were stained with the surface markers CD3 (BV605), CD4 (PE), CD8 (PercpCy5), CD14 (APCCy7) and CD19 (PEDazzle) (Biolegend) for 30 min at RT. Flow cytometric acquisition was performed on the LSR II Fortessa-4 L (BD) flow cytometer or Image stream X Mark II imaging flow cytometry (AMNIS). Flow cytometry data were analyzed using the FlowJo software (BD), Imaging flow cytometry data were analyzed using IDEAS software (Cytek Biosciences).

Nucleic acid extraction from PBMCs and tissue samples

Nucleic acid extraction was performed on tissue samples, PBMCs, and the control buffer samples (serving as negative control). Respective sequencing reads are shown in Table S2. No human DNA sequence depletion or enrichment of microbial or viral DNA was performed. PBMCs from patients with IBD, CRC or healthy individuals, tissue samples from patients with CRC or IBD as well as negative controls were all processed exactly in the same way, using the same procedures and were processed within the same batch as the patient samples and as described in the following. In detail, PBMCs and buffer samples were centrifuged for 10 min at 6000 x *g* and supernatant discarded. Microbial DNA from cell pellets and tissue samples was extracted with the ZymoBIOMICS DNA miniprep kit (Zymo Research, D4300), following the manufacturer's instructions. Instead of Zymo-Spin IICR single columns, an E-Z 96 DNA plate (Omega Bio-Tek IBD96–02) was used, and centrifugation speed was reduced to 6000 x *g*. DNA was eluted in 60 µL elution buffer and quantified using the PicoGreen dsDNA Assay (Thermo Fisher Scientific) or Pico488 dsDNA Assay (Lumiprobe).

Shotgun metagenomics sequencing

Shotgun metagenomics sequencing was performed at Microsynth AG, Balgach, CH. The library preparation utilized the Illumina TruSeq library method with unique dual indexing (UDI). Sequencing was conducted on the Illumina NovaSeq platform, specifically on the SP4 chemistry, using a paired-end 2 × 100sequencing strategy. The library preparation workflow included a comprehensive quality control (QC) step for the samples, library preparation, and a final library QC assessment. Libraries were quantified and equimolarly pooled to ensure uniform representation. The Illumina NovaSeq S4 flow cell used for DNA sequencing had a specified throughput of 16,000 million passed filter reads with an average of 30 million reads per sample (sequencing depth). We analyzed the collected metagenomics dataset using the same settings. Raw reads were trimmed for quality using fastp[57] and retained high-quality sequences, and then human host reads were subtracted by mapping the reads with the human reference genome (GRCh38) using Bowtie2.[58] Fastq files were assessed for quality control using the FASTQC application. Samples were subjected to sequencing across two distinct batches. To account for potential batch effects that could confound the analysis, we employed the ConQuR method 40, a robust statistical technique based on conditional quantile regression designed specifically for the normalization of microbiome data.

Taxonomic classification

Taxonomic classification was performed using the Kraken2 pipeline (version 2.0.8).[59] Clean reads were classified taxonomically against the PlusPF Kraken2 database using the Kraken2 classification tool with default parameters. To ensure accurate taxonomic classification, we performed a parallel taxonomic profiling analysis using MetaPhlAn4.[60] All human reads were excluded and the relative abundance was calculated based on the successful alignment against the bacteria db. Functional profiling was performed using HUMAnN3,[61] by mapping the sequences against the UniRef90 database after lowering the threshold

of intermediary taxonomy level to 0.0001. Since HUMAnN3 does not natively support paired-end reads as input, the corresponding FASTQ files were run in separate runs, and the average of matched results between forward and reverse reads were considered for further analysis.

Filtering and cleaning the data

To effectively decontaminate 7144 bacterial taxa detected in our microbiome study, especially because we involve low-biomass samples, a multi-faceted approach combining ecological plausibility, statistical analyses, and stringent experimental controls is essential. Samples were collected and processed using sterile techniques in a controlled environment, with multiple negative controls included, including water, buffer, and freezing medium (Table S2) to detect potential contamination at each stage. DNA was extracted in two different batches using different kit lots to identify batch effects. To ensure ecological plausibility, we considered only the species that were detected by 4 fold (10 reads) of average bacterial reads (2.25) in blank samples. Moreover, the species were only considered for further filtering if those were detected with more than ten reads in at least 3 patients in one of the diseases/tissues/PBMCs, reducing the species number to 738. Then we performed hierarchical correlation clustering to detect clusters with possible contamination (Figure S1A-B). Principal component analysis was used to identify and visualize batch effects. Finally, to achieve genuine signals we removed cited reagent contamination to end up with 208 species detected in biopsies and PBMCs.[26,27] Finally all the species detected were validated by MetaPhlAn4 to ensure accurate taxonomic assignment.[60]

Species specific qPCR

Quantitative real-time polymerase chain reaction (qPCR) amplification was performed using species specific primers for *Anaerostipes hadrus* (5'-CTTTAGTAGCCAGCATATAAGG −3', 5'-TTGCTCACTCTCACGAGGCT-3'),[62] *Bifidobacterium adolescentis* (5'-CTCCAGTTGGATGCATGTC-3', 5'-CGAAGGCTTGCTCCCAGT-3'),[63] *Collinsella aerofaciens* (5'-CCCGACGGGAGGGGAT-3,5'-CTTCTGCAGGTACAGTCTTGAC-3'),[64] and *Faecalibacterium prausnitzii* (5'-GGAGGAAGA AGGTCTTCGG-3', 5'-AATTCCGCCTACCTCTGCACT-3').[65] Pure bacterial DNA (DSM 23,942, DSM 20,083, DSM 3979, DSM107838) was used to perform standard curve analysis (Figure S10) and to validate primers and (Figure S11A-D). One qPCR reaction in a total volume of 10 uL consisted of 5 uL of Power SYBR Green PCR Mastermix (Thermo Fisher Scientific 4,367,659), 0.1 uL of each primer at 100 uM, nuclease free water (Promega, P119C) and the respective DNA sample. 100 ng of whole DNA (including eukaryotic and possible microbial DNA) isolated from PBMCs, adjacent CRC and CRC as well as non-inflamed and inflamed IBD tissue was used as input per reaction. We used remaining isolated DNA from the same patient samples on which previously metagenomic sequencing was performed. qPCR was run in triplicates and non-template controls (NTCs), which included the same reagents but used water in place of DNA input, were incorporated into each qPCR run. qPCR was run on Quant Studio 6 Flex (278861872) and thermal cycler settings were adapted according to the manufacturer's instructions and an annealing temperature of 68°C.

Metabolomics

Blood was collected in serum vacutainers (BD 367,896), inverted 5 times, left at least 30 min at RT for clotting and then centrifuged at 2000 x *g* for 10 minutes at RT. Subsequently obtained serum was snap frozen and stored at −80°C until further processing. Metabolomic analysis was carried out with a high-resolution mass spectrometer (Agilent QTOF 6550) described previously by Fuhrer *et al.* ,[66] and we used MetaboAnalystR package version 3.0.3 for the statistical analysis.[67] The normalized intensities by the median for each sample were mean-centered and divided by the standard deviation of each variable of all annotated features. Significance analysis was done by ANOVA followed by Tukey-HSD post-hoc analysis. Principle component analysis (PCA) was used to visualize sample variance. Heatmap visually presented the hierarchical clustering using the Euclidean method for distance calculation and Ward's linkage for clustering. Metabolite set enrichment analysis (MSEA) was carried out against the "main" data set, and a generalized linear model was used during the quantitative enrichment analysis. The correlation between the significant metabolites and enriched pathways was conducted using the corrr package in R and the sanky plot was generated using (networkD3) package.

Quantification and statistical analysis

Statistical analyses were performed in R (version 4.4.3). We employed two methods for normalization based on the type of analysis. We applied rarefaction to subsample down to 20 reads per sample for diversity analyses. Rarefaction was employed to standardize sequencing depth among samples, preventing diversity comparisons from being skewed by varying sampling efforts or sequencing depths. By establishing a minimum sequencing depth of 20 reads per sample, we ensure that only those with adequate data are considered. Given that we are identifying very low biomass, we lowered the depth to balance the retention of as many samples as possible while maintaining reliable data for thorough diversity analysis. Consequently, several samples were excluded from the analysis due to their sequencing depths not meeting the set threshold. Alpha-diversity (the number of observed genera and Chao1 indices (richness), and beta-diversity (Bray-Curtis and Jaccard dissimilarities) indices were generated using vegdist and diversity functions in the vegan R package (version 2.3–2). Principal coordinate analysis (PCoA) was performed using the phyloseq package based on the Bray-Curtis. Permutational variance analysis (PERMANOVA) was conducted using the adonis2 function from R's vegan package. Differential abundance was assessed using relative abundance. This approach accounts for the differences in total read counts between PBMC and tissue samples, enabling meaningful comparisons of bacterial composition. Either the Wilcoxon test for 2 group comparison was used or the Kruskal-Wallis test followed by Wilcoxon test for pairwise comparisons and *p* value adjusted using FDR for family error correction. Linear discriminant analysis effect size (LEFSe)[68] was used to identify differentially abundant bacteria species between two or more groups, and the linear discriminant analysis (LDA) score was obtained. The correlation between the significant metabolites and enriched pathways was conducted using the corrr package in R and the sanky plot was generated using (networkD3) package. Correlations were computed between circulating microbes and host serum metabolites using Pearson correlation coefficients implemented in the Hmisc R package. Significant associations were defined by a correlation threshold of $|r| \geq 0.4$ and an adjusted p-value < 0.05.

Acknowledgments

We thank Damina Balmer for providing editorial assistance. Flow cytometry was performed with support of the Flow Cytometry Facility, University of Zurich.

Disclosure statement

MS has shares and is co-founder of Recolony AG, Zurich, CH and has shares in PharmaBiome AG, Zurich, CH. MS served as Advisor for Abbvie, Gilead, Fresenius, Topadur, Takeda, Roche, Astra Zeneca and Celltrion. MS received speaker's honoraria from Janssen, Falk Pharma, Vifor Pharma, Pileje and Bromatech. MS received research grants from Abbvie, Takeda, Gilead, Gnubiotics, Roche, Axalbion, Pharmabiome, Topadur, Basilea, MBiomics, Storm Therapeutics, LimmatTech, Zealand Pharma, NodThera, Calypso Biotech, Menarini. Pileje, Herbodee, Vifor. GR has shares and is cofounder and head of the scientific advisory board of PharmaBiome. GR has consulted to Abbvie, Arena, Augurix, BMS, Boehringer, Calypso, Celgene, FALK, Ferring, Fisher, Genentech, Gilead, Janssen, Lilly, MSD, Novartis, Pfizer, Phadia, Roche, UCB, Takeda, Tillots, Vifor, Vital Solutions and Zeller. GR received speaker's honoraria from Abbvie, Astra Zeneca, BMS, Celgene, FALK, Janssen, MSD, Pfizer, Phadia, Takeda, Tillots, UCB, Vifor and Zeller. GR received educational grants and research grants from Abbvie, Ardeypharm, Augurix, Calypso, FALK, Flamentera, MSD, Novartis, Pfizer, Roche, Takeda, Tillots, UCB and Zeller. MT served as advisor for Topadur and Takeda. MT received speaker's honoraria from Janssen, Takeda and Intuitive Surgical. RF has served as an Advisor or speaker for Roche, Pierre Fabre Pharma, Servier, Bristol Myers Squibb, Merck Sharp&Dome, Astra Zeneca. LB has served as advisor for Abbvie, Amgen, BMS, Falk, Janssen, Pfizer, Lilly, Takeda, Sanofi, Esocap, Aquilion and received speaker fees from Takeda, Sanofi, Abbvie, Janssen, Lilly, Falk, BMS, Pfizer. The additional authors declare that they have no competing interests relevant to this work.

Funding

This work was supported by the Stiftung Experimentelle Biomedizin (MS), Swiss National Science Foundation grant No 320030_184753 (MS),Swiss National Science Foundation grant No 320030E_190969 (MS), The Swiss Cancer League grant no. KFS-5372-08-2021-R (MS), Research grant from the Fondazione San Salvatore (MS), Research grant from the Stiftung fürwissenschaftliche Forschung an der Universität Zürich grant No STWF-22-009 (MS),

Research grant from the ISREC Foundation (MS, ICA), Lighthouse project grant of the Comprehensive Cancer Center Zurich (CCCZ) and University Medicine Zurich (UMZH) (MS), Wilhelm-Sander Foundation grant no. 2021.104.1 (MS), Research grant from the Iten-Kohaut Foundation (BH), Research grant from the Universityof Zürich "Forschungskredit" (BH), Research grant from Novartis Foundation formedical-biological Research (BH), Research grant from the Fond'Action contre lecancer (BH). SB was supported by a Walter and Gertrud SiegenthalerFellowship, a grant from the Hartmann Mueller Foundation and a fellowship fromthe Fonds zur Foerderung des Akademischen Nachwuchses, University of Zurich.

ORCID

Yasser Morsy http://orcid.org/0000-0001-8234-1877
Michael Scharl http://orcid.org/0000-0002-6729-1469

Author contributions

Conceptualization: YM, PW, MW, ÅW, MS
Methodology: YM, PW, AN, LT, ÅW, BH, RM, SS, CG, SL, LB, NZ, MS
Investigation: ÅW, PW, BH, LT, CM, AN, EG, RM, CG, SL, SB, GR, MT, MR, HP, ICA, NZ, SZ, AE, JHN, PH, AK, RF, MGM, YM, MS
Visualization: YM, ÅW, PW
Funding acquisition: MS, BH, ICA, SB
Project administration: MS
Supervision: BH, MGM, MS
Writing – original draft: YM, ÅW, MS
Writing – review & editing: All authors

Data and code availability

Sequencing data (fastq) have been deposited at NCBI Home – BioProject – NCBI (nih.gov) or at the European Nucleotide Archive (ENA). They are publicly available as of the publication date under the accession number PRJNA1024674 (https://www.ncbi.nlm.nih.gov/bioproject/1024674). Metabolomics data has been deposited at MassIVE and is publicly available as of the date of publication under accession number MSV000095692. Sup plementary tables can be found under the following link for the reviewer's reference https://www.biorxiv.org/content/10.1101/2024.12.16.628609v1. The link is also cited within the manuscript as ref[25].

Materials availability

This study did not generate new unique reagents.

References

1. Hou K, Wu Z X, Chen X Y, Wang J Q, Zhang D, Xiao C, Zhu D, Koya JB, Wei L, Li J, et al. Microbiota in health and diseases. Signal Transduct Targeted Ther. 2022;7(1):135. doi: 10.1038/s41392-022-00974-4.
2. Zhang Y, Zhang L, Zheng S, Li M, Xu C, Jia D, Qi Y, Hou T, Wang L, Wang B, et al. Fusobacterium nucleatum promotes colorectal cancer cells adhesion to endothelial cells and facilitates extravasation and metastasis by inducing ALPK1/NF-kappaB/ICAM1 axis. Gut Microbes. 2022;14(1):2038852. doi: 10.1080/19490976.2022.2038852.
3. Pleguezuelos-Manzano C, Puschhof J, Rosendahl Huber A, van Hoeck A, Wood HM, Nomburg J, Gurjao C, Manders F, Dalmasso G, Stege PB, et al. Mutational signature in colorectal cancer caused by genotoxic pks(+) E. coli. Nature. 2020;580(7802):269–273. doi: 10.1038/s41586-020-2080-8.
4. Galeano Nino JL, Wu H, LaCourse KD, Kempchinsky AG, Baryiames A, Barber B, Futran N, Houlton J, Sather C, Sicinska E, et al. Effect of the intratumoral microbiota on spatial and cellular heterogeneity in cancer. Nature. 2022;611(7937):810–817. doi: 10.1038/s41586-022-05435-0.
5. Zheng D, Liwinski T, Elinav E. Interaction between microbiota and immunity in health and disease. Cell Res. 2020;30(6):492–506. doi: 10.1038/s41422-020-0332-7.
6. Anderson NM, Simon MC. The tumor microenvironment. Curr Biol CB. 2020;30(16):R921–R925. doi: 10.1016/j.cub.2020.06.081.

7. Shan Y, Lee M, Chang EB. The gut microbiome and inflammatory bowel diseases. Annu Rev Med. 2022;73 (1):455–468. doi: 10.1146/annurev-med-042320-021020.
8. Bullman S, Pedamallu CS, Sicinska E, Clancy TE, Zhang X, Cai D, Neuberg D, Huang K, Guevara F, Nelson T, et al. Analysis of Fusobacterium persistence and antibiotic response in colorectal cancer. Science. 2017;358 (6369):1443–1448. doi: 10.1126/science.aal5240.
9. Tan CCS, Ko KKK, Chen H, Liu J, Loh M, Chia M, Nagarajan N. No evidence for a common blood microbiome based on a population study of 9,770 healthy humans. Nat Microbiol. 2023;8(5):973–985. doi: 10.1038/s41564-023-01350-w.
10. Xu X, Ocansey DKW, Hang S, Wang B, Amoah S, Yi C, Zhang X, Liu L, Mao F. The gut metagenomics and metabolomics signature in patients with inflammatory bowel disease. Gut Pathog. 2022;14(1):26. doi: 10.1186/s13099-022-00499-9.
11. Proctor LM, Creasy HH, Fettweis JM, Lloyd-Price J, Mahurkar A, Zhou W, Buck GA, Snyder MP, Strauss JF, Weinstock GM, et al. The integrative human microbiome project. Nature. 2019;569(7758):641–648. doi: 10.1038/s41586-019-1238-8.
12. Huttenhower C. Structure, function and diversity of the healthy human microbiome. Nature. 2012;486:207–214. doi: 10.1038/nature11234.
13. Methé BA. A framework for human microbiome research. Nature. 2012;486:215–221. doi: 10.1038/nature11209.
14. Forbes JD, Van Domselaar G, Bernstein CN. Microbiome survey of the inflamed and Noninflamed gut at different compartments within the gastrointestinal tract of inflammatory bowel disease patients. Inflamm Bowel Dis. 2016;22(4):817–825. doi: 10.1097/MIB.0000000000000684.
15. Darfeuille-Michaud A, Boudeau J, Bulois P, Neut C, Glasser A-L, Barnich N, Bringer M-A, Swidsinski A, Beaugerie L, Colombel J-F, et al. High prevalence of adherent-invasive Escherichia coli associated with ileal mucosa in Crohn's disease. Gastroenterology. 2004;127(2):412–421. doi: 10.1053/j.gastro.2004.04.061.
16. Read E, Curtis MA, Neves JF. The role of oral bacteria in inflammatory bowel disease. Nat Rev Gastroenterol Hepatol. 2021;18(10):731–742. doi: 10.1038/s41575-021-00488-4.
17. Montalban-Arques A, Katkeviciute E, Busenhart P, Bircher A, Wirbel J, Zeller G, Morsy Y, Borsig L, Glaus Garzon JF, Müller A, et al. Commensal clostridiales strains mediate effective anti-cancer immune response against solid tumors. Cell Host & Microbe. 2021;29(10):1573–1588.e7. doi: 10.1016/j.chom.2021.08.001.
18. Kostic AD, Chun E, Robertson L, Glickman J, Gallini C, Michaud M, Clancy T, Chung D, Lochhead P, Hold G, et al. Fusobacterium nucleatum potentiates intestinal tumorigenesis and modulates the tumor-immune microenvironment. Cell Host & Microbe. 2013;14(2):207–215. doi: 10.1016/j.chom.2013.07.007.
19. Wirbel J, Pyl PT, Kartal E, Zych K, Kashani A, Milanese A, Fleck JS, Voigt AY, Palleja A, Ponnudurai R, et al. Meta-analysis of fecal metagenomes reveals global microbial signatures that are specific for colorectal cancer. Nat Med. 2019;25(4):679–689. doi: 10.1038/s41591-019-0406-6.
20. Thomas AM, Manghi P, Asnicar F, Pasolli E, Armanini F, Zolfo M, Beghini F, Manara S, Karcher N, Pozzi C, et al. Metagenomic analysis of colorectal cancer datasets identifies cross-cohort microbial diagnostic signatures and a link with choline degradation. Nat Med. 2019;25(4):667–678. doi: 10.1038/s41591-019-0405-7.
21. Dejea CM, Fathi P, Craig JM, Boleij A, Taddese R, Geis AL, Wu X, destefano Shields CE, Hechenbleikner EM, Huso DL, et al. Patients with familial adenomatous polyposis harbor colonic biofilms containing tumorigenic bacteria. Science. 2018;359(6375):592–597. doi: 10.1126/science.aah3648.
22. Bertocchi A, Carloni S, Ravenda PS, Bertalot G, Spadoni I, Lo Cascio A, Gandini S, Lizier M, Braga D, Asnicar F, et al. Gut vascular barrier impairment leads to intestinal bacteria dissemination and colorectal cancer metastasis to liver. Cancer Cell. 2021;39(5):708–724.e11. doi: 10.1016/j.ccell.2021.03.004.
23. Messaritakis I, Vogiatzoglou K, Tsantaki K, Ntretaki A, Sfakianaki M, Koulouridi A, Tsiaoussis J, Mavroudis D, Souglakos J. The prognostic value of the detection of microbial translocation in the blood of colorectal cancer patients. Cancers (Basel). 2020;12(4):1058. doi: 10.3390/cancers12041058.
24. Kitamura T, Qian BZ, Pollard JW. Immune cell promotion of metastasis. Nat Rev Immunol. 2015;15(2):73–86. doi: 10.1038/nri3789.
25. Morsy Y. Blood-borne immune cells carry low biomass DNA remnants of microbes in patients with colorectal cancer or inflammatory bowel disease. bioRxiv. 2024; 628609. doi: 10.1101/2024.12.16.628609.
26. de Goffau MC, Lager S, Salter SJ, Wagner J, Kronbichler A, Charnock-Jones DS, Peacock SJ, Smith GCS, Parkhill J. Recognizing the reagent microbiome. Nat Microbiol. 2018;3(8):851–853. doi: 10.1038/s41564-018-0202-y.
27. Kennedy KM, de Goffau MC, Perez-Muñoz ME, Arrieta M-C, Bäckhed F, Bork P, Braun T, Bushman FD, Dore J, de Vos WM, et al. Questioning the fetal microbiome illustrates pitfalls of low-biomass microbial studies. Nature. 2023;613(7945):639–649. doi: 10.1038/s41586-022-05546-8.
28. Zhai W, Wu F, Zhang Y, Fu Y, Liu Z. The immune escape mechanisms of mycobacterium tuberculosis. Int J Mol Sci. 2019;20(2):340. doi: 10.3390/ijms20020340.
29. Eisele NA, Ruby T, Jacobson A, Manzanillo P, Cox J, Lam L, Mukundan L, Chawla A, Monack D. Salmonella require the fatty acid regulator PPARdelta for the establishment of a metabolic environment essential for long-term persistence. Cell Host & Microbe. 2013;14(2):171–182. doi: 10.1016/j.chom.2013.07.010.

30. Amar J, Chabo C, Waget A, Klopp P, Vachoux C, Bermúdez-Humarán LG, Smirnova N, Bergé M, Sulpice T, Lahtinen S, et al. Intestinal mucosal adherence and translocation of commensal bacteria at the early onset of type 2 diabetes: molecular mechanisms and probiotic treatment. EMBO Mol Med. 2011;3(9):559–572. doi: 10.1002/emmm.201100159.
31. Abed J, Maalouf N, Manson AL, Earl AM, Parhi L, Emgård JEM, Klutstein M, Tayeb S, Almogy G, Atlan KA, et al. Colon cancer-associated Fusobacterium nucleatum May originate from the oral cavity and reach colon tumors via the circulatory system. Front Cell Infect Microbiol. 2020;10:400. doi: 10.3389/fcimb.2020.00400.
32. Gihawi A, Ge Y, Lu J, Puiu D, Xu A, Cooper CS, Brewer DS, Pertea M, Salzberg SL. Major data analysis errors invalidate cancer microbiome findings. mBio. 2023;14(5):e0160723. doi: 10.1128/mbio.01607-23.
33. Geller LT, Barzily-Rokni M, Danino T, Jonas OH, Shental N, Nejman D, Gavert N, Zwang Y, Cooper ZA, Shee K, et al. Potential role of intratumor bacteria in mediating tumor resistance to the chemotherapeutic drug gemcitabine. Science. 2017;357(6356):1156–1160. doi: 10.1126/science.aah5043.
34. Amann RI, Binder BJ, Olson RJ, Chisholm SW, Devereux R, Stahl DA. Combination of 16S rRNA-targeted oligonucleotide probes with flow cytometry for analyzing mixed microbial populations. Appl Environ Microbiol. 1990;56(6):1919–1925. doi: 10.1128/aem.56.6.1919-1925.1990.
35. Markman JL, Shiao SL. Impact of the immune system and immunotherapy in colorectal cancer. J Gastrointest Oncol. 2015;6(2):208–223. doi: 10.3978/j.issn.2078-6891.2014.077.
36. Ai D, Pan H, Li X, Gao Y, Liu G, Xia LC. Identifying gut microbiota associated with colorectal cancer using a zero-inflated lognormal model. Front Microbiol. 2019;10:826. doi: 10.3389/fmicb.2019.00826.
37. Salazar AM, Aparicio R, Clark RI, Rera M, Walker DW. Intestinal barrier dysfunction: an evolutionarily conserved hallmark of aging. Dis Model Mech. 2023;16(4). doi: 10.1242/dmm.049969.
38. Ghosh TS, Shanahan F, O'Toole PW. The gut microbiome as a modulator of healthy ageing. Nat Rev Gastroenterol Hepatol. 2022;19(9):565–584. doi: 10.1038/s41575-022-00605-x.
39. Lloyd-Price J, Arze C, Ananthakrishnan AN, Schirmer M, Avila-Pacheco J, Poon TW, Andrews E, Ajami NJ, Bonham KS, Brislawn CJ, et al. Multi-omics of the gut microbial ecosystem in inflammatory bowel diseases. Nature. 2019;569(7758):655–662. doi: 10.1038/s41586-019-1237-9.
40. Human Microbiome Project C. Structure, function and diversity of the healthy human microbiome. Nature. 2012;486:207–214. doi: 10.1038/nature11234.
41. Kim MY, Gaspal FMC, Wiggett HE, McConnell FM, Gulbranson-Judge A, Raykundalia C, Walker LSK, Goodall MD, Lane PJL. CD4(+)CD3(-) accessory cells costimulate primed CD4 T cells through OX40 and CD30 at sites where T cells collaborate with B cells. Immunity. 2003;18(5):643–654. doi: 10.1016/s1074-7613(03)00110-9.
42. Parel Y, Chizzolini C. CD4+ CD8+ double positive (DP) T cells in health and disease. Autoimmun Rev. 2004;3(3):215–220. doi: 10.1016/j.autrev.2003.09.001.
43. Desfrancois J, Moreau-Aubry A, Vignard V, Godet Y, Khammari A, Dréno B, Jotereau F, Gervois N. Double positive CD4CD8 alphabeta T cells: a new tumor-reactive population in human melanomas. PLOS ONE. 2010;5(1):e8437. doi: 10.1371/journal.pone.0008437.
44. Quandt D, Rothe K, Scholz R, Baerwald CW, Wagner U, Frey O. Peripheral CD4CD8 double positive T cells with a distinct helper cytokine profile are increased in rheumatoid arthritis. PLOS ONE. 2014;9(3):e93293. doi: 10.1371/journal.pone.0093293.
45. Baba T, Ishizu A, Iwasaki S, Suzuki A, Tomaru U, Ikeda H, Yoshiki T, Kasahara M. CD4+/CD8+ macrophages infiltrating at inflammatory sites: a population of monocytes/macrophages with a cytotoxic phenotype. Blood. 2006;107(5):2004–2012. doi: 10.1182/blood-2005-06-2345.
46. Pallett LJ, Swadling L, Diniz M, Maini AA, Schwabenland M, Gasull AD, Davies J, Kucykowicz S, Skelton JK, Thomas N. Tissue CD14(+)CD8(+) T cells reprogrammed by myeloid cells and modulated by LPS. Nature. 2023;614(7947):334–342. doi: 10.1038/s41586-022-05645-6.
47. Mutignani M, Penagini R, Gargari G, Guglielmetti S, Cintolo M, Airoldi A, Leone P, Carnevali P, Ciafardini C, Petrocelli G, et al. Blood bacterial DNA load and profiling differ in colorectal cancer patients compared to tumor-free controls. Cancers (Basel). 2021;13(24):6363. doi: 10.3390/cancers13246363.
48. Katkeviciute E, Bircher A, Sanchez R, Schwill M, Dorst A, Morsy Y, Conde J, Zamboni N, Gademann K, Scharl M, et al. Bacteria-derived 3-hydroxydodecanoic acid induces a potent anti-tumor immune response via the GPR84 receptor. Cell Rep. 2025;44(3):115357. doi: 10.1016/j.celrep.2025.115357.
49. Liu D, Xie L-S, Lian S, Li K, Yang Y, Wang W-Z, Hu S, Liu S-J, Liu C, He Z, et al. Anaerostipes hadrus, a butyrate-producing bacterium capable of metabolizing 5-fluorouracil. mSphere. 2024;9(4):e0081623. doi: 10.1128/msphere.00816-23.
50. Vujkovic-Cvijin I, Welles HC, Ha CWY, Huq L, Mistry S, Brenchley JM, Trinchieri G, Devkota S, Belkaid Y. The systemic anti-microbiota IgG repertoire can identify gut bacteria that translocate across gut barrier surfaces. Sci Transl Med. 2022;14(658):eabl3927. doi: 10.1126/scitranslmed.abl3927.
51. Genua F, Raghunathan V, Jenab M, Gallagher WM, Hughes DJ. The role of gut barrier dysfunction and microbiome dysbiosis in colorectal cancer development. Front Oncol. 2021;11:626349. doi: 10.3389/fonc.2021.626349.

52. Choi Y, Lichterman JN, Coughlin LA, Poulides N, Li W, Del Valle P, Palmer SN, Gan S, Kim J, Zhan X, et al. Immune checkpoint blockade induces gut microbiota translocation that augments extraintestinal antitumor immunity. Sci Immunol. 2023;8(81):eabo2003. doi: 10.1126/sciimmunol.abo2003.
53. Turner JR. Intestinal mucosal barrier function in health and disease. Nat Rev Immunol. 2009;9(11):799–809. doi: 10.1038/nri2653.
54. Plovier H, Everard A, Druart C, Depommier C, Van Hul M, Geurts L, Chilloux J, Ottman N, Duparc T, Lichtenstein L, et al. A purified membrane protein from Akkermansia muciniphila or the pasteurized bacterium improves metabolism in obese and diabetic mice. Nat Med. 2017;23(1):107–113. doi: 10.1038/nm.4236.
55. Wang J, Jelcic I, Mühlenbruch L, Haunerdinger V, Toussaint NC, Zhao Y, Cruciani C, Faigle W, Naghavian R, Foege M, et al. HLA-DR15 molecules jointly shape an Autoreactive T cell repertoire in multiple sclerosis. Cell. 2020;183(5):1264–1281.e20. doi: 10.1016/j.cell.2020.09.054.
56. Naghavian R, Faigle W, Oldrati P, Wang J, Toussaint NC, Qiu Y, Medici G, Wacker M, Freudenmann LK, Bonté P-E, et al. Microbial peptides activate tumour-infiltrating lymphocytes in glioblastoma. Nature. 2023;617(7962):807–817. doi: 10.1038/s41586-023-06081-w.
57. Chen S, Zhou Y, Chen Y, Gu J. Fastp: an ultra-fast all-in-one FASTQ preprocessor. Bioinformatics. 2018;34(17):i884–i890. doi: 10.1093/bioinformatics/bty560.
58. Langmead B, Wilks C, Antonescu V, Charles R, Hancock J. Scaling read aligners to hundreds of threads on general-purpose processors. Bioinformatics. 2019;35(3):421–432. doi: 10.1093/bioinformatics/bty648.
59. Wood DE, Lu J, Langmead B. Improved metagenomic analysis with Kraken 2. Genome Biology. 2019;20(1):257. doi: 10.1186/s13059-019-1891-0.
60. Blanco-Miguez A, Beghini F, Cumbo F, McIver LJ, Thompson KN, Zolfo M, Manghi P, Dubois L, Huang KD, Thomas AM, et al. Extending and improving metagenomic taxonomic profiling with uncharacterized species using MetaPhlAn 4. Nat Biotechnol. 2023;41(11):1633–1644. doi: 10.1038/s41587-023-01688-w.
61. Beghini F, McIver LJ, Blanco-Míguez A, Dubois L, Asnicar F, Maharjan S, Mailyan A, Manghi P, Scholz M, Thomas AM, et al. Integrating taxonomic, functional, and strain-level profiling of diverse microbial communities with bioBakery 3. Elife. 2021;10. doi: 10.7554/eLife.65088.
62. Louis P, Young P, Holtrop G, Flint HJ. Diversity of human colonic butyrate-producing bacteria revealed by analysis of the butyryl-CoA: acetate CoA-transferase gene. Environ Microbiol. 2010;12(2):304–314. doi: 10.1111/j.1462-2920.2009.02066.x.
63. Matsuki T, Watanabe K, Tanaka R, Oyaizu H. Rapid identification of human intestinal bifidobacteria by 16S rRNA-targeted species- and group-specific primers. FEMS Microbiol Lett. 1998;167(2):113–121. doi: 10.1111/j.1574-6968.1998.tb13216.x.
64. Kassinen A, Krogius-Kurikka L, Mäkivuokko H, Rinttilä T, Paulin L, Corander J, Malinen E, Apajalahti J, Palva A. The fecal microbiota of irritable bowel syndrome patients differs significantly from that of healthy subjects. Gastroenterology. 2007;133(1):24–33. doi: 10.1053/j.gastro.2007.04.005.
65. Ramirez-Farias C, Slezak K, Fuller Z, Duncan A, Holtrop G, Louis P. Effect of inulin on the human gut microbiota: stimulation of bifidobacterium adolescentis and faecalibacterium prausnitzii. Br J Nutr. 2009;101(4):541–550. doi: 10.1017/S0007114508019880.
66. Fuhrer T, Heer D, Begemann B, Zamboni N. High-throughput, accurate mass metabolome profiling of cellular extracts by flow injection-time-of-flight mass spectrometry. Anal Chem. 2011;83(18):7074–7080. doi: 10.1021/ac201267k.
67. Pang Z, Chong J, Li S, Xia J. MetaboAnalystR 3.0: toward an optimized workflow for global metabolomics. Metabolites. 2020;10(5):186. doi: 10.3390/metabo10050186.
68. Segata N, Izard J, Waldron L, Gevers D, Miropolsky L, Garrett WS, Huttenhower C. Metagenomic biomarker discovery and explanation. Genome Biol. 2011;12(6):R60. doi: 10.1186/gb-2011-12-6-r60.